Supporting Information for

A *meso*-acyl-BODIPY-based fluorogenic probe for the selective monitoring of aldo-keto reductase 1C1 in living cells

Yeri Kim,[‡a] Le Bich Hang Pham,[‡b] Jae Yeol Lee,[a] Jeeyeon Lee[*b] and Youngmi Kim[*a]

[a]*Department of Chemistry and Research Institute of Basic Sciences, Kyung Hee University, 26 Kyungheedae-ro, Dongdaemun-gu, Seoul, 02447, Korea.*

[b]*Research Institute of Pharmaceutical Sciences, College of Pharmacy, Seoul National University, 1 Gwanak-ro, Gwanak-gu, Seoul 08826, Korea.*

youngmi.kim@khu.ac.kr
jyleeut@snu.ac.kr

Table of Contents:

Experimental Materials

Materials

All chemicals were purchased commercially and used as received without further purification. All solvents were spectral grade unless otherwise noted. Flash column chromatography was performed using silica gel (38−75 μm), which was supplied from Qingdao Meigao Chem. Co., Ltd (Chengyang, China). Aqueous solutions were freshly prepared with deionized water from a water purification system (Younglin Corp. Korea). Anhydrous dichloromethane, Dess-Martin periodinane (DMP), and β-nicotinamide adenine dinucleotide phosphate reduced tetrasodium salt (NADPH) were purchased from ThermoFisher Scientific Co. (Waltham, MA). Hydrochloric acid (35.0%~37.0%), sodium bicarbonate concentrate ($NaHCO_3$), sodium thiosulfate ($Na_2S_2O_3$) and magnesium sulfate ($MgSO_4$) were obtained from Samchun Chemicals (Korea). Acetone was obtained from Daejung Chemicals (Korea). Phenylmagnesium bromide (1.0 M in THF) was purchased from Sigma-Aldrich Co. Inc. (Saint Louis, MO). **2**,[1] **1-OH**,[2] **1-CO**,[2] and **3**[3] were prepared as described in the literature.[1-3]

General methods, instrumentation and measurements

NMR (^1H and ^{13}C) spectra were recorded on a JEOL 500 MHz and Bruker 400 MHz spectrometers. The ^1H and ^{13}C chemical shifts (δ) were reported in parts per million (ppm), referenced to the residual solvent resonances. Splitting patterns are denoted as s (singlet), d (doublet), t (triplet), q (quartet), m (multiplet), and br (broad). High-resolution electrospray ionization (ESI) mass spectra were obtained at the Korea Basic Science Institute (KBSI). Electrospray ionization mass spectra (ESI-MS) was carried out using a Waters ACQUITY Arc system equipped with a photodiode array (PDA) detector. Separation was performed on a Waters XBridge C18 column (4.6 × 50 mm, 3.5 μm). UV/Vis absorption spectra were obtained on a SCINCO UV S-3100 spectrophotometer. Fluorescence measurements were recorded on a Hitachi F-7100 fluorescence spectrophotometer using quartz cuvettes with a path length of 1 cm and TECAN INFINITE M PLEX microplate reader using glass-based 96-well plates. Fluorescence quantum yields were determined by the integrating sphere method on an absolute PL (photoluminescence) quantum yield measurement system (Hamamatsu C11347-11, Hamamatsu, Japan).

1. Synthesis of Compounds

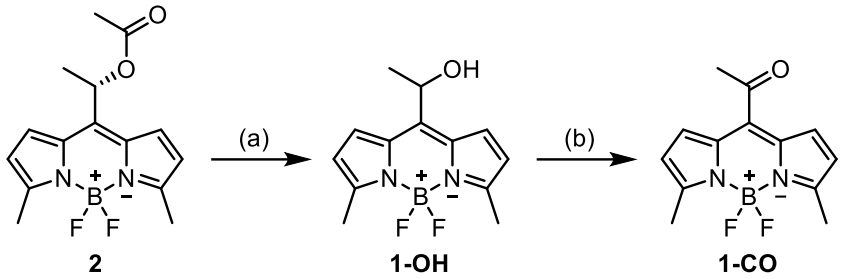

Scheme S1. Synthetic scheme for **1-OH** and **1-CO**. (a) 2 M HCl, acetone, 50 °C , 21 h, 57%. (b) Dess-Martin periodinane, dry CH_2Cl_2, 0 °C to r.t., 2 h, 48%.

1-OH.[1] To a stirred solution of **2**[1] (80 mg, 0.26 mmol) in acetone (12 mL) at room temperature under a nitrogen atmosphere was added 2 M HCl (8 mL). After the mixture was stirred at 50 ℃ for 21 hours, the resulting mixture was cooled to room temperature. The crude mixture was diluted with CH_2Cl_2 (20 mL) and washed three times with saturated $NaHCO_3$ solution (10 mL × 3). The collected organic layers were dried over anhydrous $MgSO_4$, filtered, and evaporated under reduced pressure. The crude product was purified by column chromatography on silica gel using 25:1 hexanes:dichloromethane as the mobile phase to afford **1-OH** as a dark brown solid (39 mg, 57%). ^{1}H NMR (500 MHz, $CDCl_3$): δ = 7.36 (d, J = 4.0 Hz, 2H), 6.25 (d, J = 4.0 Hz, 2H), 5.27 (q, J = 6.7Hz, 1H), 2.59 (s, 6H), 2.26 (s,1H), 1.65 (d, J = 6.9 Hz, 3H); ^{13}C-NMR (125 MHz, $CDCl_3$): δ = 157.6, 146.8, 132.4, 128.1, 119.3, 67.5, 29.9, 26.7, 15.0.

1-CO.[1] To a stirred solution of **1-OH** (60 mg, 0.23 mmol) in dry CH_2Cl_2 (5 mL) at 0 °C under a nitrogen atmosphere was added Dess-Martin periodinane (145 mg, 0.34 mmol) in dry CH_2Cl_2 (6 mL) at 0 ℃. After the mixture was stirred at room temperature for 2 hours, the resulting mixture was quenched with saturated $Na_2S_2O_3$ solution. The crude mixture was diluted with CH_2Cl_2 (20 mL) and washed three times with saturated $NaHCO_3$ solution (10 mL × 3). The collected organic layers were dried over anhydrous $MgSO_4$, filtered, and evaporated under reduced pressure. The crude product was purified by column chromatography on silica gel using 25:1:0.04 hexanes:dichloromethane:ethyl acetate as the mobile phase to afford **1-CO** as a purple solid (29 mg, 48%). ^{1}H NMR (500 MHz, CD_2Cl_2): δ = 6.89 (d, J =4.0 Hz, 2H), 6.33 (d, J = 4.0 Hz, 2H), 2.61 (s, 3H), 2.57 (s, 6H); ^{13}C-NMR (125 MHz, $CDCl_3$): δ = 198.7, 160.2, 138.9, 131.0, 128.8, 120.7, 32.9, 15.2; HR-MS (ESI) m/z: $[M+Na]^+$ calcd for $C_{13}H_{13}BF_2N_2ONa$, 285.0981; found 285.0983.

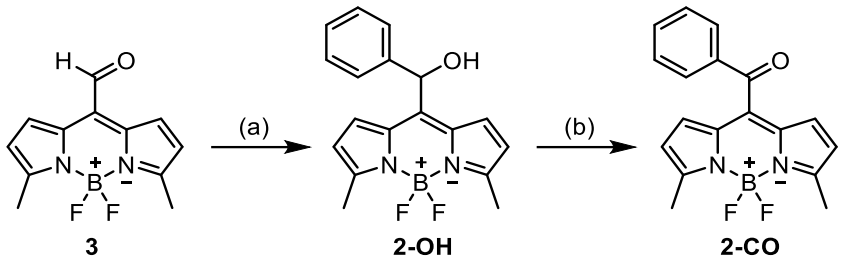

Scheme S2. Synthetic scheme for **2-OH** and **2-CO**. (a) i) dry CH_2Cl_2, phenylmagnesium bromide (1.0 M in THF), 0 °C to r.t., 4 h, 80%. (b) Dess-Martin periodinane, dry CH_2Cl_2, 0 °C to r.t., 2 h, 37%.

2-OH. To a stirred solution of **3**[3] (50 mg, 0.2 mmol) in dry CH_2Cl_2 (10 mL) at 0 °C under a nitrogen atmosphere was added phenylmagnesium bromide (1.0 M in THF) (0.4 mL) at 0 °C. After the mixture was stirred at room temperature for 4 hours, the resulting mixture was quenched with water. The crude mixture was diluted with CH_2Cl_2 (20 mL) and washed three times with water (10 mL × 3). The collected organic layers were dried over anhydrous $MgSO_4$, filtered, and evaporated under reduced pressure. The crude product was purified by column chromatography on silica gel using 10:1 hexanes:ethyl acetate as the mobile phase to afford **2-OH** as a orange solid (52 mg, 80%). ^{1}H NMR (500 MHz, CD_2Cl_2): δ = 7.46 (d, J = 7.4 Hz, 2H), 7.34-7.29 (m, 4H), 7.25 (t, J = 7.4 Hz, 1H), 6.26 (d, J = 4.0 Hz, 2H), 6.21 (s, 1H), 2.53 (s, 6H); ^{13}C-NMR (100 MHz, CD_2Cl_2): δ = 157.9, 143.3, 141.9, 133.1, 129.1, 128.6, 127.9, 125.6, 119.5, 71.9, 29.7, 14.7; HR-MS (ESI) m/z: $[M+H]^+$ calcd for $C_{18}H_{18}BF_2N_2O$, 327.1475; found 327.1480.

2-CO. To a stirred solution of **2-OH** (50 mg, 0.15 mmol) in dry CH_2Cl_2 (10 mL) at 0 °C under a nitrogen atmosphere was added Dess-Martin periodinane (96 mg, 0.23 mmol) in dry CH_2Cl_2 (5 mL) at 0 °C. After the mixture was stirred at room temperature for 2 hours, the resulting mixture was quenched with saturated $Na_2S_2O_3$ solution. The crude mixture was diluted with CH_2Cl_2 (20 mL) and washed three times with saturated $NaHCO_3$ solution (10 mL × 3). The collected organic layers were dried over anhydrous $MgSO_4$, filtered, and evaporated under reduced pressure. The crude product was purified by column chromatography on silica gel using 10:1 hexanes:dichloromethane as the mobile phase to afford **2-CO** as a pink solid (18 mg, 38%). ^{1}H NMR (500 MHz, CD_2Cl_2): δ = 7.95 (dd, J = 8.6, 1.1 Hz, 2H), 7.66-7.62 (m, 1H), 7.48-7.45 (m, 2H), 6.64 (d, J = 4.6 Hz, 2H), 6.25 (d, J = 4.6 Hz, 2H), 2.59 (s, 6H); ^{13}C-NMR (100 MHz, CD_2Cl_2): δ = 191.3, 159.7, 137.5, 136.6, 134.9, 132.4, 130.2, 129.2, 128.8, 120.4, 29.7, 14.8; HR-MS (ESI) m/z: $[M+H]^+$ calcd for $C_{18}H_{16}BN_2OF_2$, 325.1318; found 325.1324.

2. Photophysical Properties of Compounds

(a) Absorption and fluorescence emission spectra of compounds in phosphate buffer (10 mM, pH 7.4, 1% DMSO)

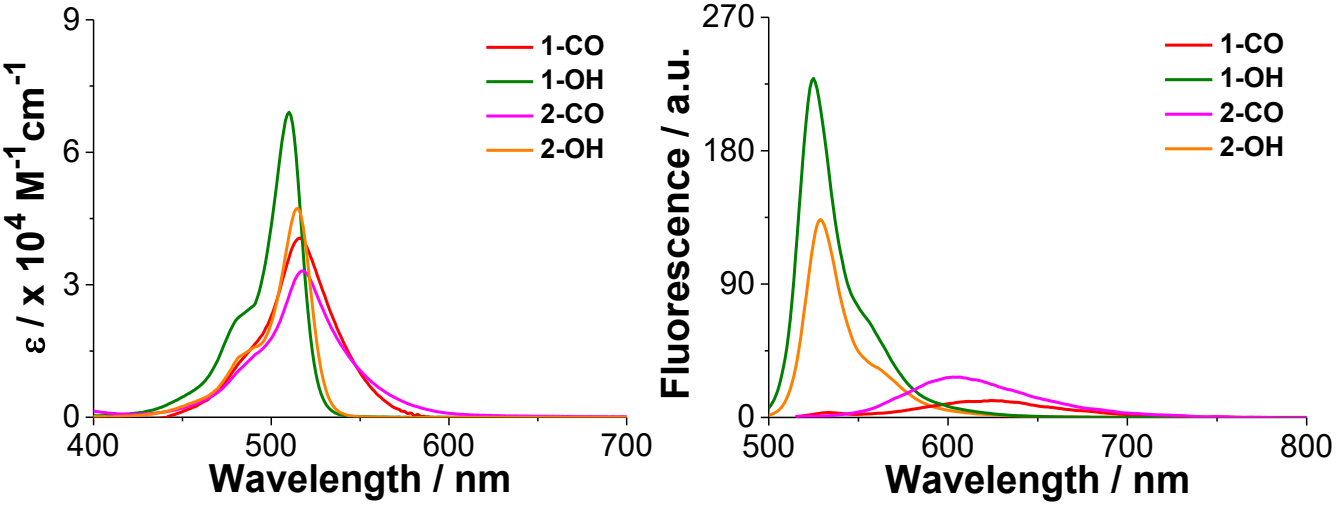

Figure S1. UV-Vis absorption (left) and fluorescence emission (right) spectra of compounds in phosphate buffer (10 mM, pH 7.4, 1% DMSO) at 25 °C. Excited at 500 nm (**1-CO** and **2-CO**) and at 470 nm (**1-OH** and **2-OH**). Emission spectra of **1-CO** and **2-CO** are magnified 20-fold for clarity. [compound] = 10 μM.

Table S1. Comparison of photophysical properties of compounds in phosphate buffer (10 mM, pH 7.4, 1% DMSO) at 25 °C.

Compounds	$\lambda_{abs.\ max}$ [nm]	ε^a [$M^{-1}cm^{-1}$]	$\lambda_{em.\ max}{}^b$ [nm]	Φ_{FL}
1-CO	516	40,000	624	0.011
1-OH	510	69,000	525	0.840
2-CO	518	33,000	603	0.033
2-OH	515	47,000	529	0.826

[a]Measured at each absorption maximum. [b]Excited at 500 nm (**1-CO** and **2-CO**) and 470 nm (**1-OH** and **2-OH**).

(b) Absorption and fluorescence emission spectra of 1-CO in DMSO-water mixtures

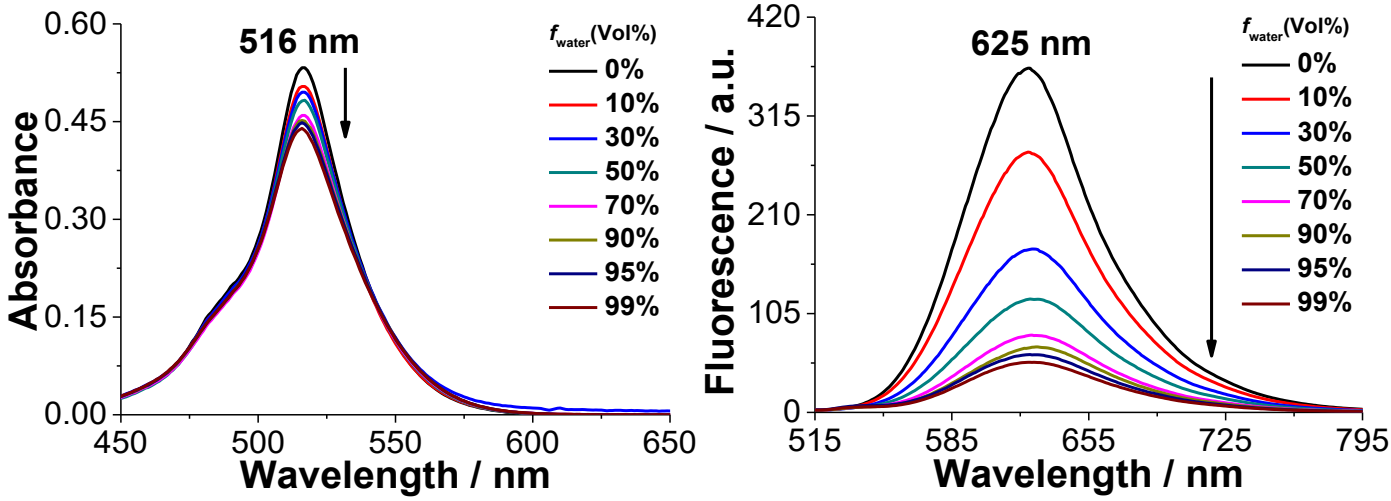

Figure S2. Absorption (left) and fluorescence emission (right) spectra of **1-CO** in DMSO-water mixtures with different water fraction (f_{water} (vol%); 0, 10, 30, 50, 70, 90, 99%) at 25 °C. Excited at 500 nm. [**1-CO**] = 10 μM.

(c) Absorption and fluorescence emission spectra of 2-CO in DMSO-water mixtures

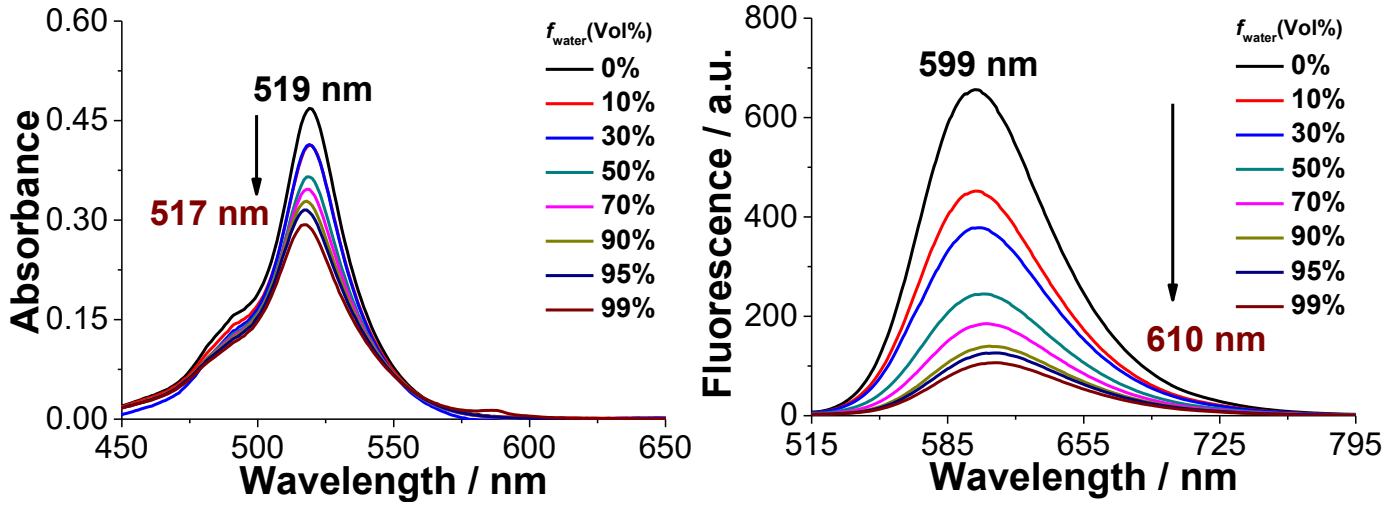

Figure S3. Absorption (left) and fluorescence emission (right) spectra of **2-CO** in DMSO-water mixtures with different water fraction (f_{water} (vol%); 0, 10, 30, 50, 70, 90, 99%) at 25 °C. Excited at 500 nm. [**2-CO**] = 10 μM.

(d) Absorption and fluorescence emission spectra of 1-CO in dioxane-water mixtures

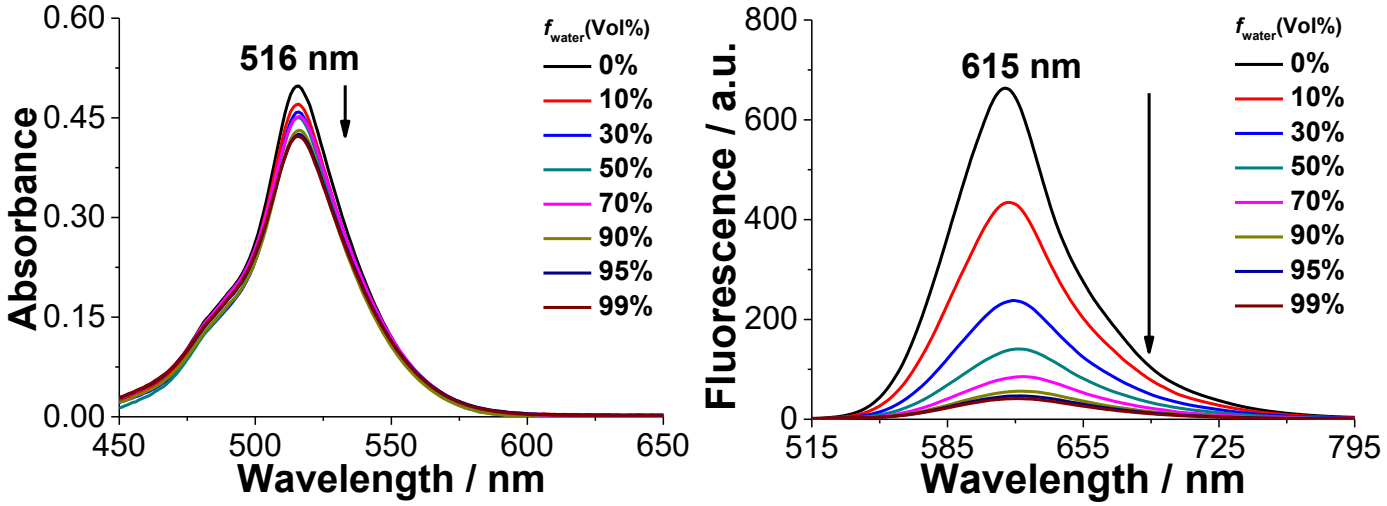

Figure S4. Absorption (left) and fluorescence emission (right) spectra of **1-CO** in dioxane-water mixtures with different water fraction (f_{water} (vol%); 0, 10, 30, 50, 70, 90, 99%) at 25 °C. Excited at 500 nm. [**1-CO**] = 10 μM.

(e) Absorption and fluorescence emission spectra of 2-CO in dioxane-water mixtures

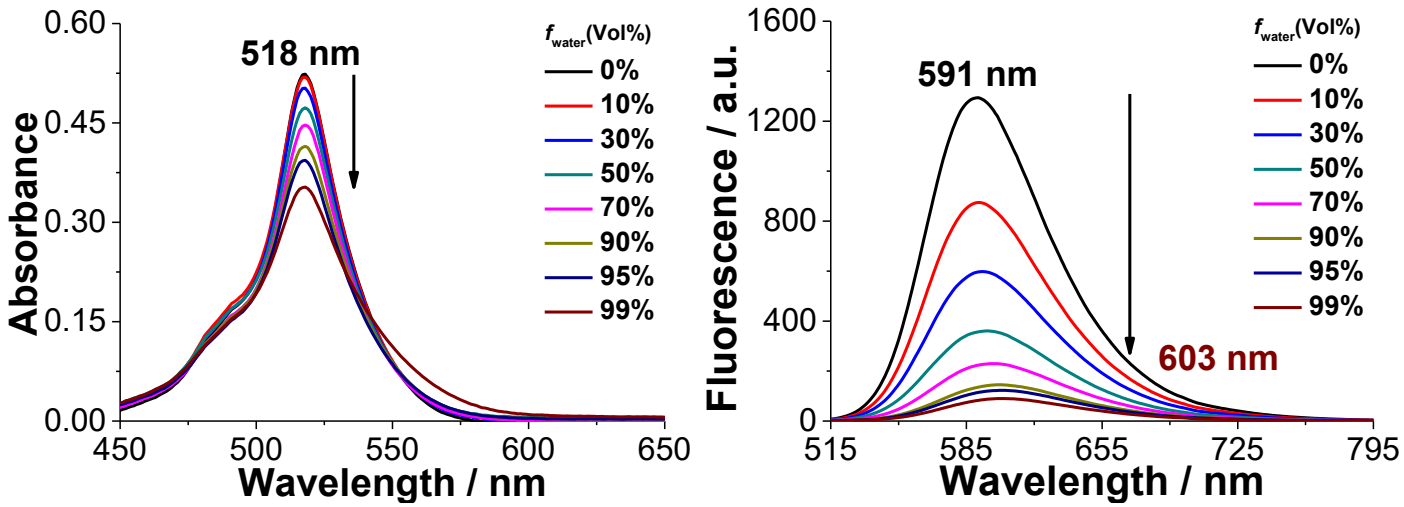

Figure S5. Absorption (left) and fluorescence emission (right) spectra of **2-CO** in dioxane-water mixtures with different water fraction (f_{water} (vol%); 0, 10, 30, 50, 70, 90, 99%) at 25 °C. Excited at 500 nm. [**2-CO**] = 10 μM.

(f) Absorption and fluorescence emission spectra of 1-OH in DMSO-water mixtures

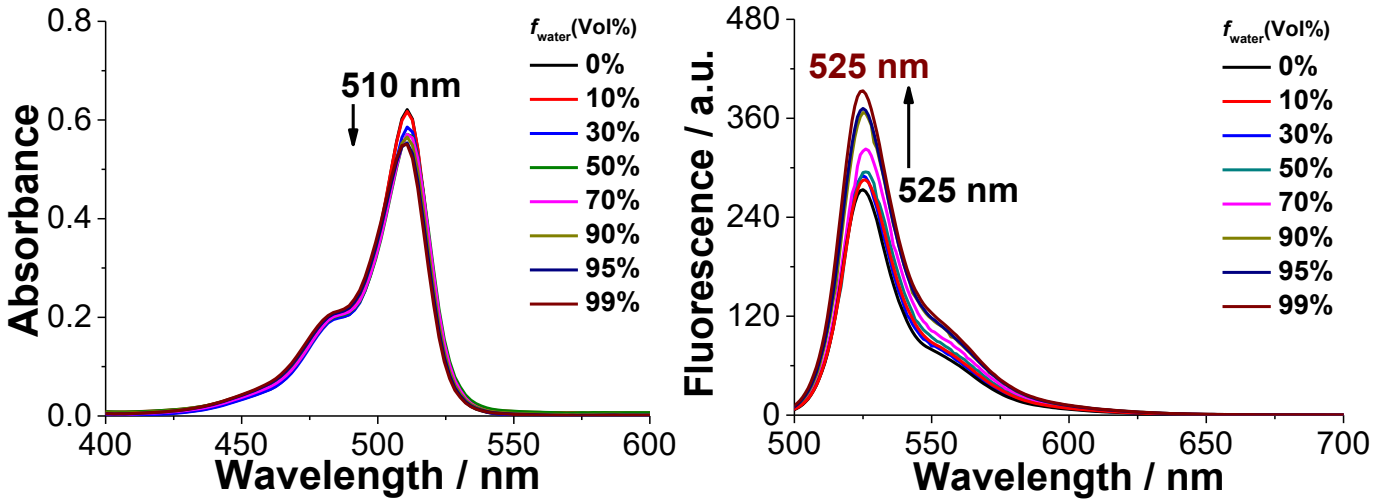

Figure S6. Absorption (left) and fluorescence emission (right) spectra of **1-OH** in DMSO-water mixtures with different water fraction (f_{water} (vol%); 0, 10, 30, 50, 70, 90, 99%) at 25 °C. Excited at 470 nm. [**1-OH**] = 10 μM.

(g) Absorption and fluorescence emission spectra of 2-OH in DMSO-water mixtures

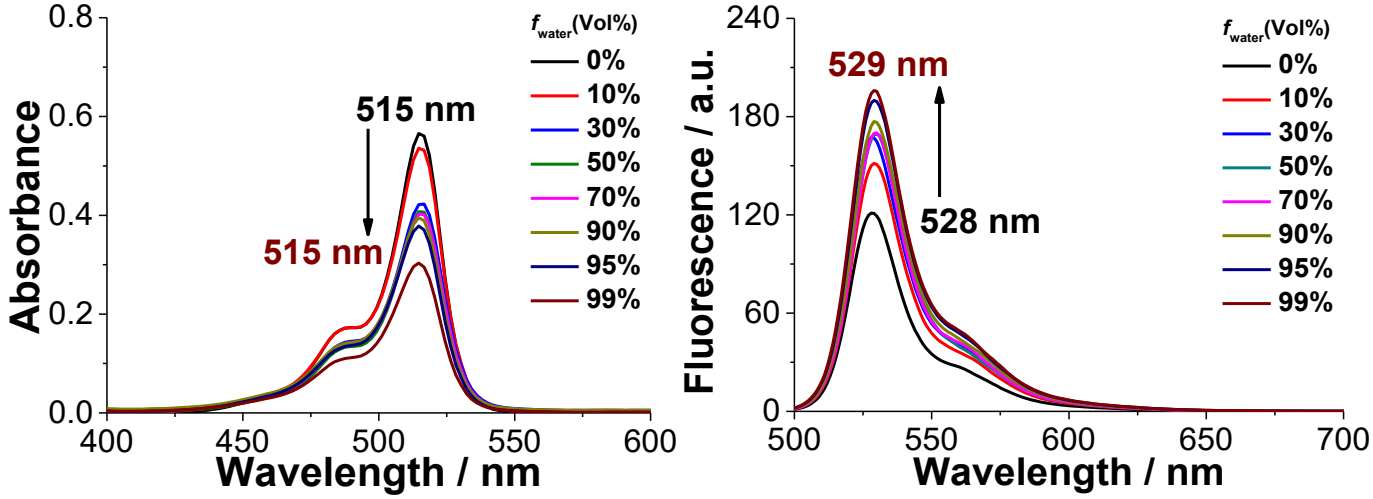

Figure S7. Absorption (left) and fluorescence emission (right) spectra of **2-OH** in DMSO-water mixtures with different water fraction (f_{water} (vol%); 0, 10, 30, 50, 70, 90, 99%) at 25 °C. Excited at 470 nm. [**2-OH**] = 10 μM.

(h) Absorption and fluorescence emission spectra of 1-CO in various organic solvents

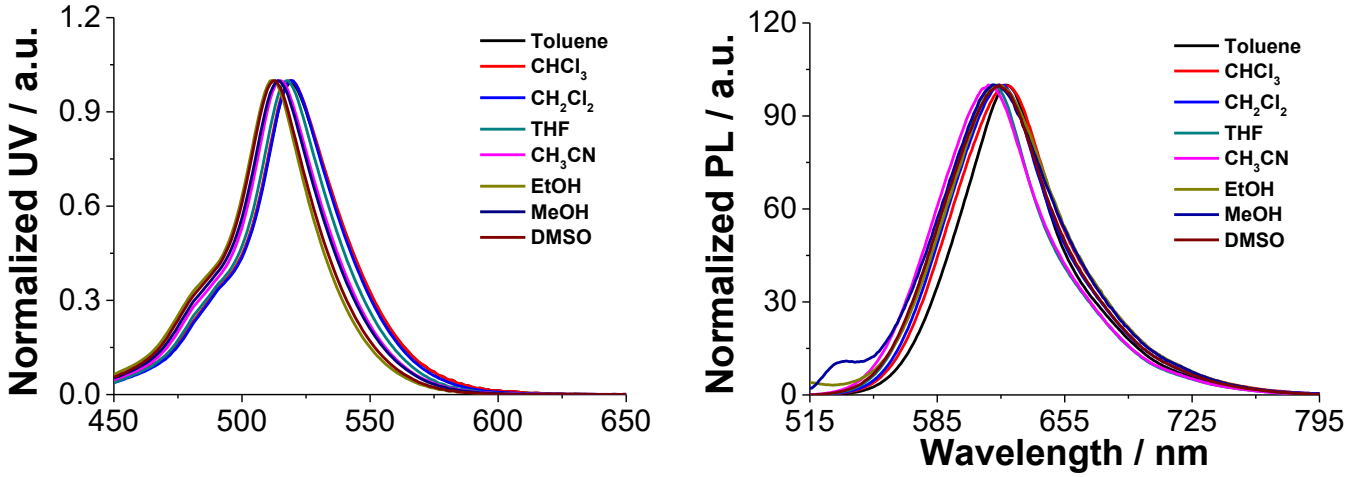

Figure S8. Normalized absorption (left) and fluorescence emission (right) spectra of **1-CO** in various solvents at 25 °C. Excited at 500 nm. [**1-CO**] = 10 μM. (Reproduced from *Org. Lett.*, 2025, **27**, 6710)

3. Confirmation of Spectral Changes of 1-CO and 2-CO by $NaBH_4$

(a) Absorption and fluorescence emission spectra of compounds in water:EtOH (9:1, 25 °C)

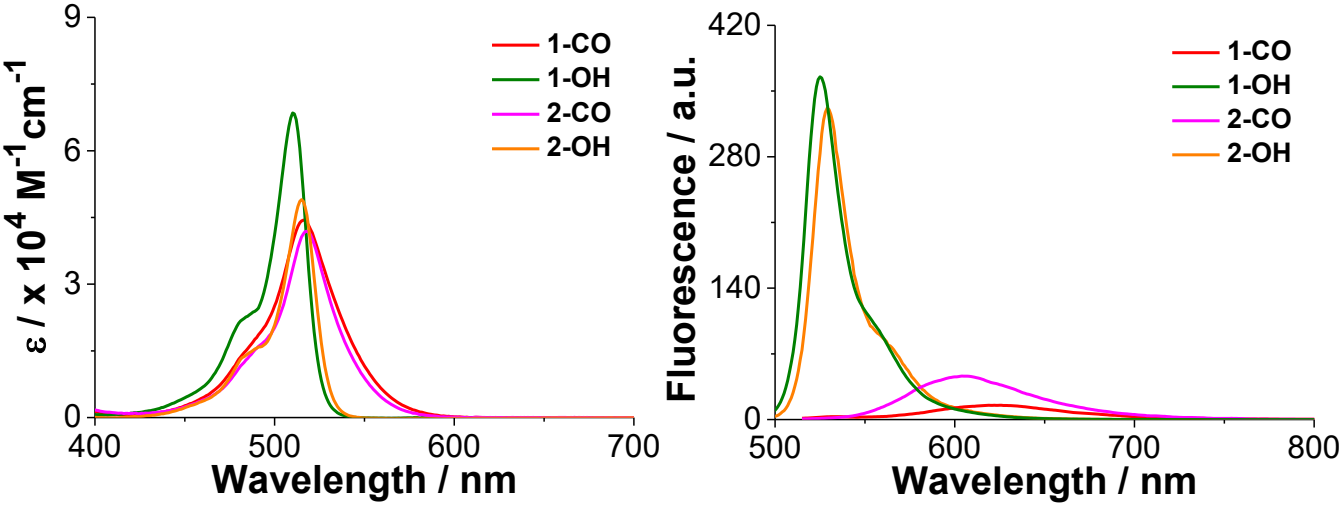

Figure S9. UV-Vis absorption (left) and fluorescence emission (right) spectra of compounds in water:EtOH (9:1) at 25 °C. Excited at 500 nm (**1-CO** and **2-CO**) and at 470 nm (**1-OH** and **2-OH**). Emission spectra of **1-CO** and **2-CO** are magnified 20-fold for clarity. [compound] = 10 μM.

Table S2. Comparison of photophysical properties of compounds in water:EtOH (9:1) at 25 °C.

Compounds	$\lambda_{abs.\ max}$ [nm]	ε^a [$M^{-1}cm^{-1}$]	$\lambda_{em.\ max}{}^b$ [nm]	Φ_{FL}
1-CO	516	44,000	619	0.008
1-OH	511	69,000	525	0.833
2-CO	518	42,000	606	0.023
2-OH	515	49,000	529	0.815

[a]Measured at each absorption maximum. [b]Excited at 500 nm (**1-CO** and **2-CO**) and 470 nm (**1-OH** and **2-OH**).

(b) Monitoring spectral changes of 1-CO upon addition of $NaBH_4$ in water:EtOH (9:1, 25 °C)

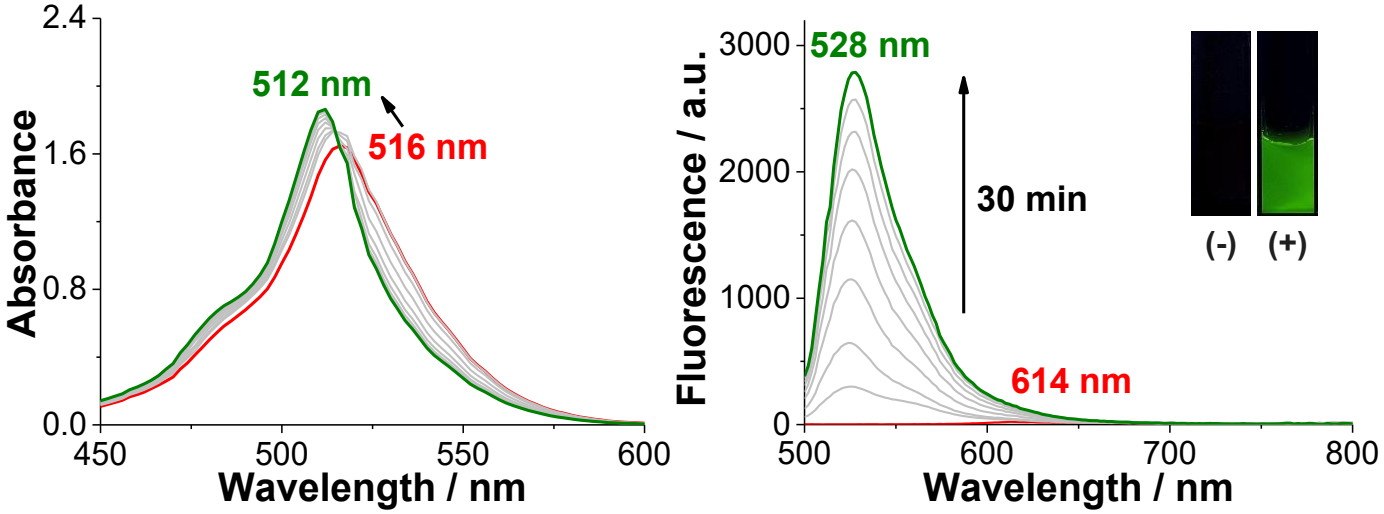

Figure S10. Absorbance (left) and time-dependent fluorescence emission (right) spectra of **1-CO** (10 μM) upon incubation with $NaBH_4$ (5 equiv.) in water:EtOH (9:1) at 25 °C. Spectra were obtained every 5 min over 30 min (λ_{ex} = 470 nm). The red and green lines indicate the spectra of **1-CO** before and after 30 min incubation with $NaBH_4$, respectively.

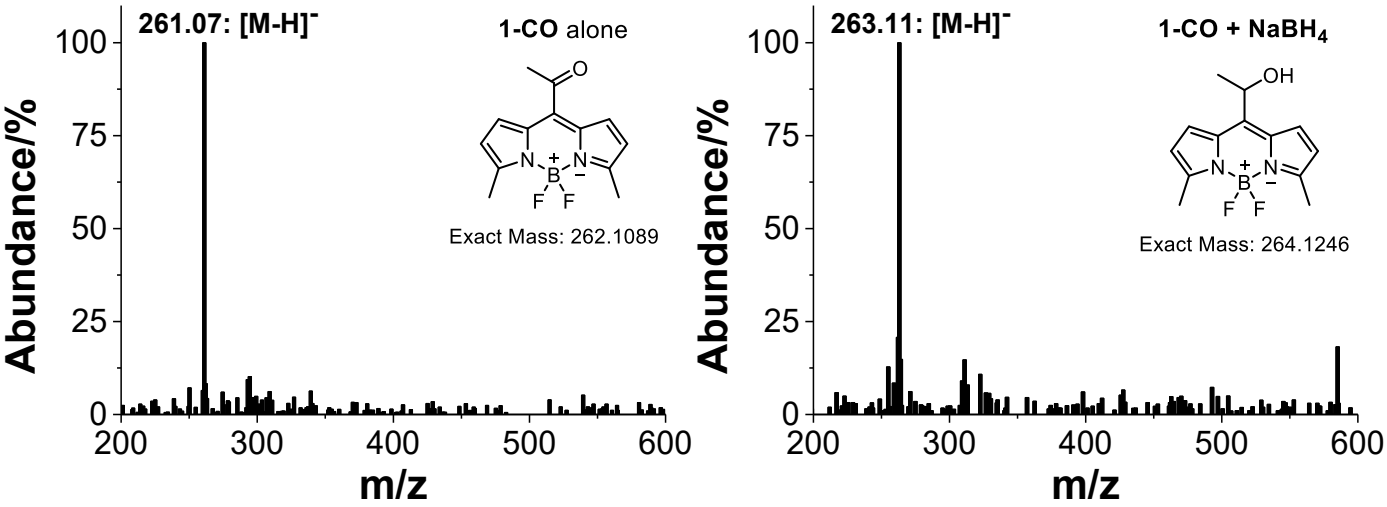

Figure S11. ESI-MS spectra (negative mode) of **1-CO** (10 μM) in water:EtOH (9:1) before (left) and after (right) treatment with $NaBH_4$ (5 equiv.) for 30 min at 25 °C. The samples were analyzed isocratically at a ratio of solvent A (water) 40% and solvent B (acetonitrile) 60% for 10 min, with a flow rate of 0.5 mL/min. (left) ESI-MS spectrum of **1-CO** alone showed the peak at *m/z* 261.07, which corresponds to $[M-H]^-$ for **1-CO**. (right) ESI-MS spectrum of **1-CO** after treatment with $NaBH_4$ (10 equiv.) for 30 min showed the peak at *m/z* 263.11, which corresponds to $[M-H]^-$ for the reduction product, **1-OH**.

(c) Monitoring spectral changes of 2-CO upon addition of $NaBH_4$ in water:EtOH (9:1, 25 °C)

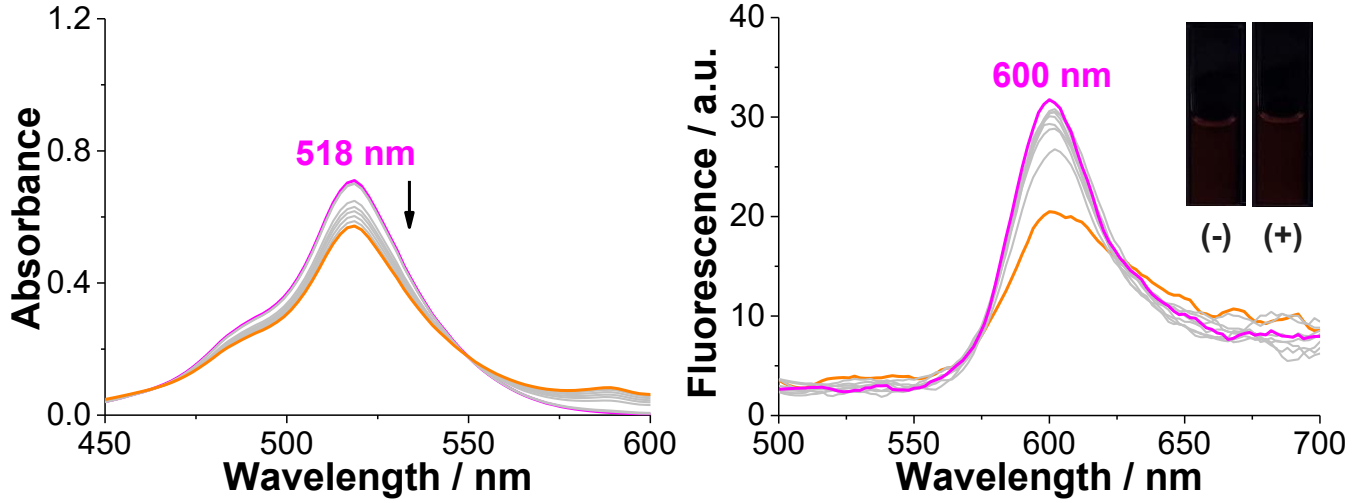

Figure S12. Time-dependent fluorescence emission spectra of **2-CO** (10 μM) upon incubation with $NaBH_4$ (5 equiv.) in water:EtOH (9:1) at 25 °C. Spectra were obtained every 5 min over 30 min (λ_{ex} = 470 nm). The pink and orange lines indicate the spectra of **2-CO** before and after 30 min incubation with $NaBH_4$, respectively.

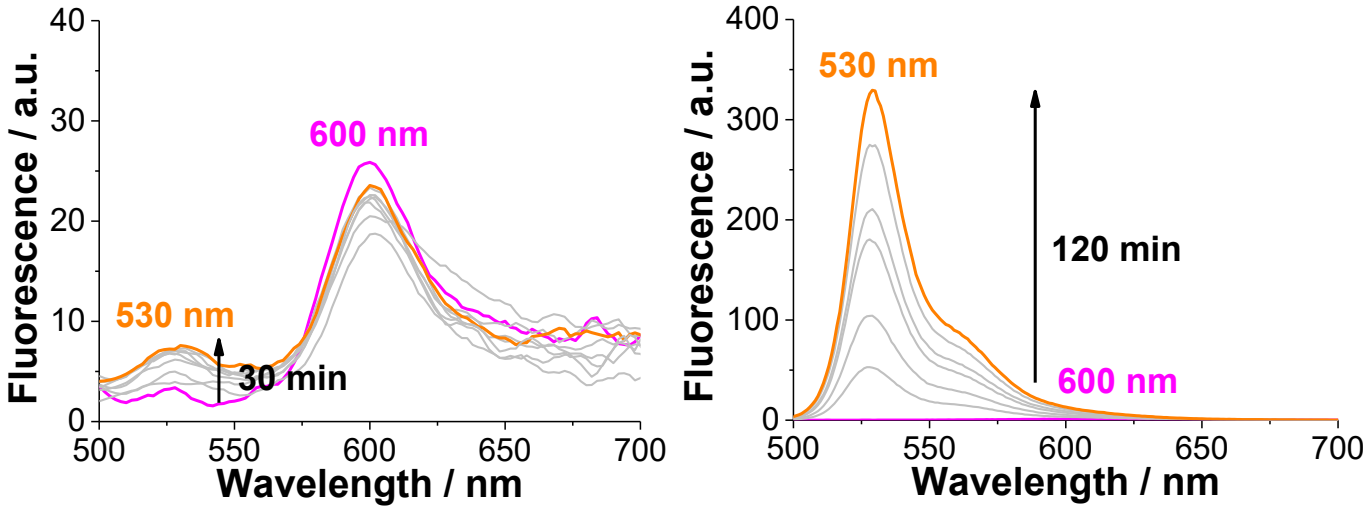

Figure S13. Time-dependent fluorescence emission spectra of **2-CO** (10 μM) upon incubation with $NaBH_4$ (10 equiv., left) and $NaBH_4$ (50 equiv., right) in water:EtOH (9:1) at 25 °C. Spectra were obtained every 5 min over 30 min (left) and 20 min over 2 hour (right) (λ_{ex} = 470 nm). The pink and orange lines indicate the spectra of **2-CO** before and after 30 min incubation with $NaBH_4$, respectively.

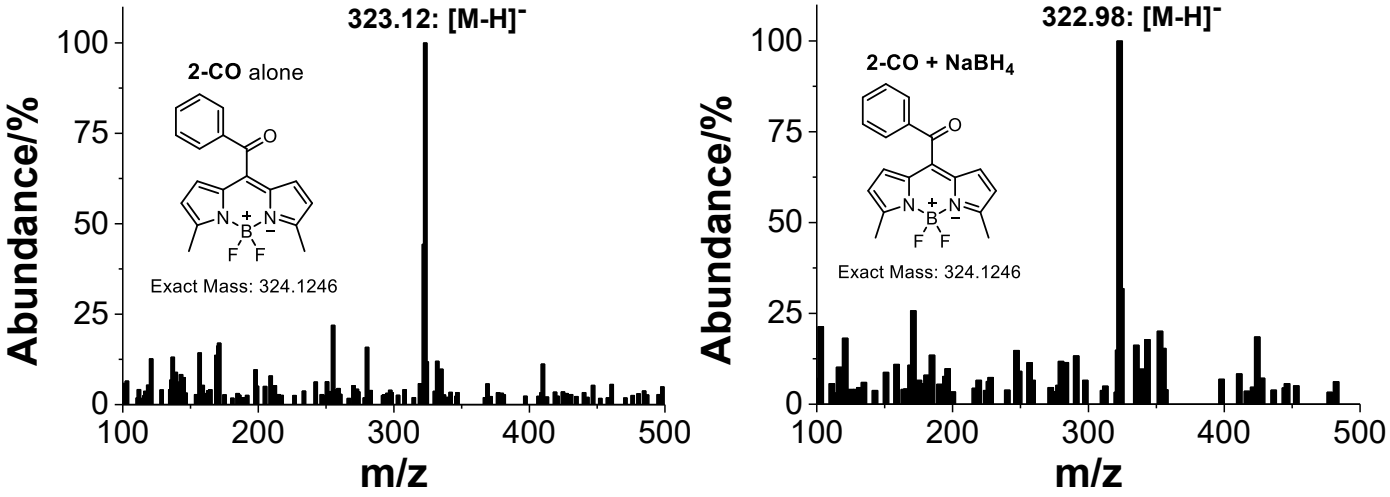

Figure S14. ESI-MS spectra (negative mode) of **2-CO** (10 μM) in water:EtOH (9:1) before (left) and after (right) treatment with $NaBH_4$ (5 equiv.) for 30 min at 25 °C. The samples were analyzed isocratically at a ratio of solvent A (water) 40% and solvent B (acetonitrile) 60% for 10 min, with a flow rate of 0.5 mL/min. (left) ESI-MS spectrum of **2-CO** alone showed the peak at *m*/*z* 323.12, which corresponds to $[M-H]^-$ for **2-CO**. (right) ESI-MS spectrum of **2-CO** after treatment with $NaBH_4$ (10 equiv.) for 30 min showed the peak at *m*/*z* 322.98, which corresponds to $[M-H]^-$ for **2-CO**.

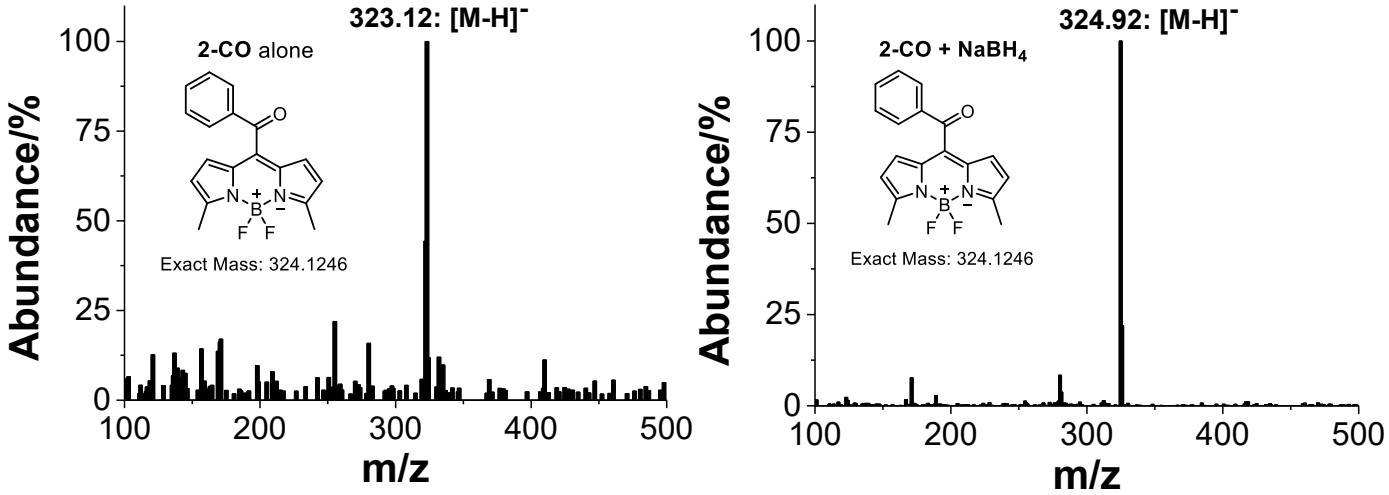

Figure S15. ESI-MS spectra (negative mode) of **2-CO** (10 μM) in water:EtOH (9:1) before (left) and after (right) treatment with $NaBH_4$ (50 equiv.) for 2 hour at 25 °C. The samples were analyzed isocratically at a ratio of solvent A (water) 40% and solvent B (acetonitrile) 60% for 10 min, with a flow rate of 0.5 mL/min. (left) ESI-MS spectrum of **2-CO** alone showed the peak at *m*/*z* 323.12, which corresponds to $[M-H]^-$ for **2-CO**. (right) ESI-MS spectrum of **2-CO** after treatment with $NaBH_4$ (10 equiv.) for 30 min showed the peak at *m*/*z* 324.92, which corresponds to $[M-H]^-$ for **2-OH**.

4. Enzymatic Sensing Response of *meso*-Acyl Probes (1-CO and 2-CO)

(a) Enzymatic sensing response of 1-CO and its isoform selectivity

*Time-dependent emission spectral changes of **1-CO** without and with NADPH*

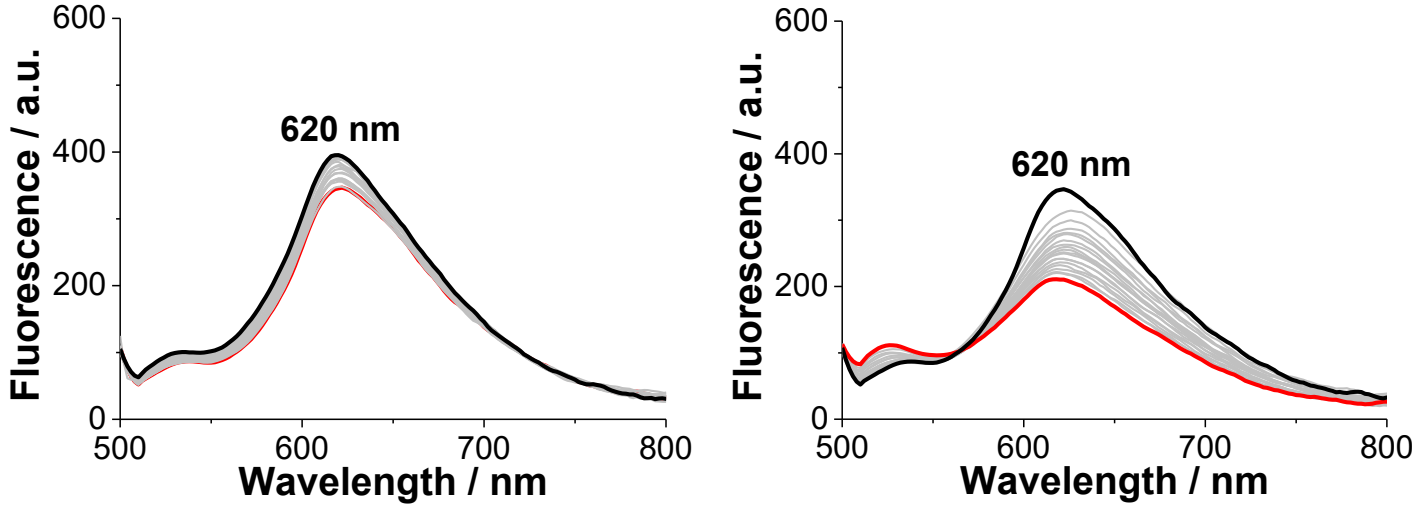

Figure S16. Time-dependent emission spectra of **1-CO** (4 μM) in the absence (left) and presence (right) of NADPH (50 μM). All measurements were performed in phosphate buffer (10 mM, pH 7.4, 1% DMSO) at 37 °C. Spectra were obtained every 20 min over 6 h (λ_{ex} = 470 nm). Black and red lines indicate the spectra of **1-CO** before and after 6 h incubation, respectively.

*Time-dependent emission spectral changes of **1-CO** with AKR1C1/NADPH and AKR1C2/ NADPH*

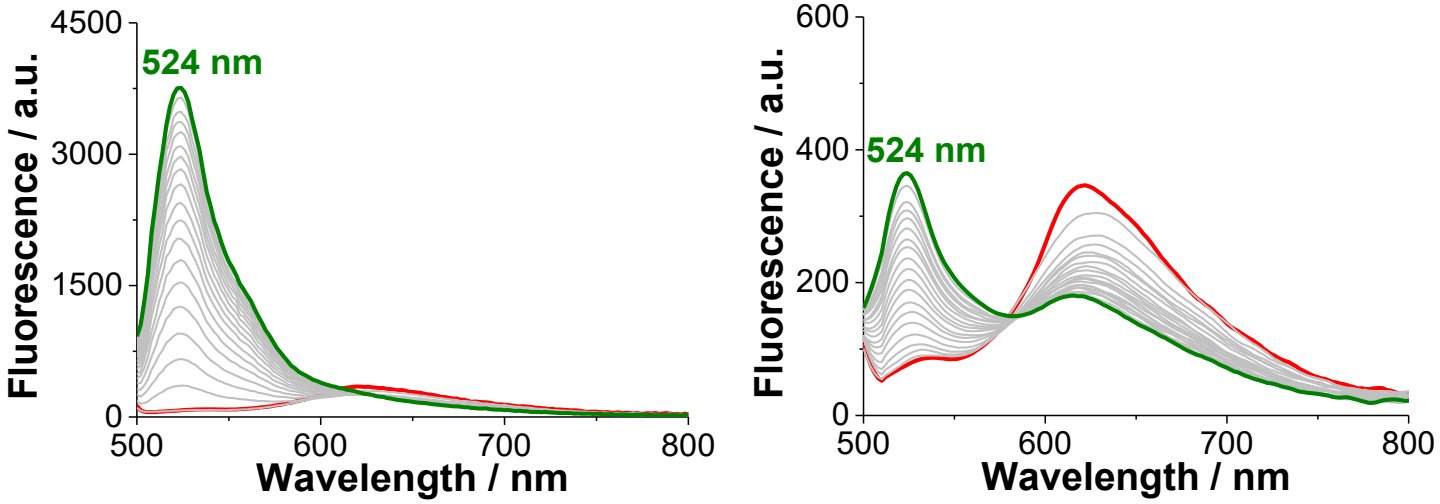

Figure S17. Time-dependent emission spectra of **1-CO** (4 μM) upon incubation with AKR1C1 (100 nM, left) and AKR1C2 (100 nM, right) in phosphate buffer (10 mM, pH 7.4, 1% DMSO, 50 μM NADPH) at 37 °C. Spectra were obtained every 20 min over 6 h (λ_{ex} = 470 nm). Red and green lines indicate the spectra of **1-CO** before and after 6 h incubation with AKR1C1 (left) and AKR1C2 (right), respectively.

*Time-dependent emission spectral changes of **1-CO** with AKR1C3/NADPH and AKR1C4/ NADPH*

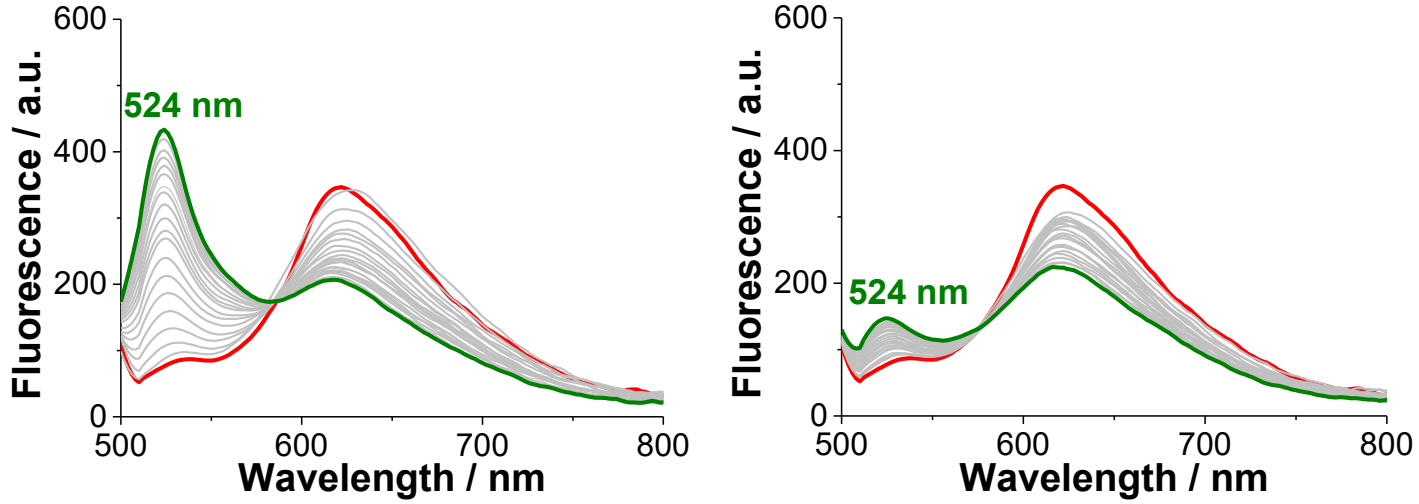

Figure S18. Time-dependent emission spectra of **1-CO** (4 μM) upon incubation with AKR1C3 (100 nM, left) and AKR1C4 (100 nM, right) in phosphate buffer (10 mM, pH 7.4, 1% DMSO, 50 μM NADPH) at 37 °C. Spectra were obtained every 20 min over 6 h (λ_{ex} = 470 nm). Red and green lines indicate the spectra of **1-CO** before and after 6 h incubation with AKR1C3 (left) and AKR1C4 (right), respectively.

*Comparative fluorescence turn-on responses of **1-CO** toward AKR1C isoforms*

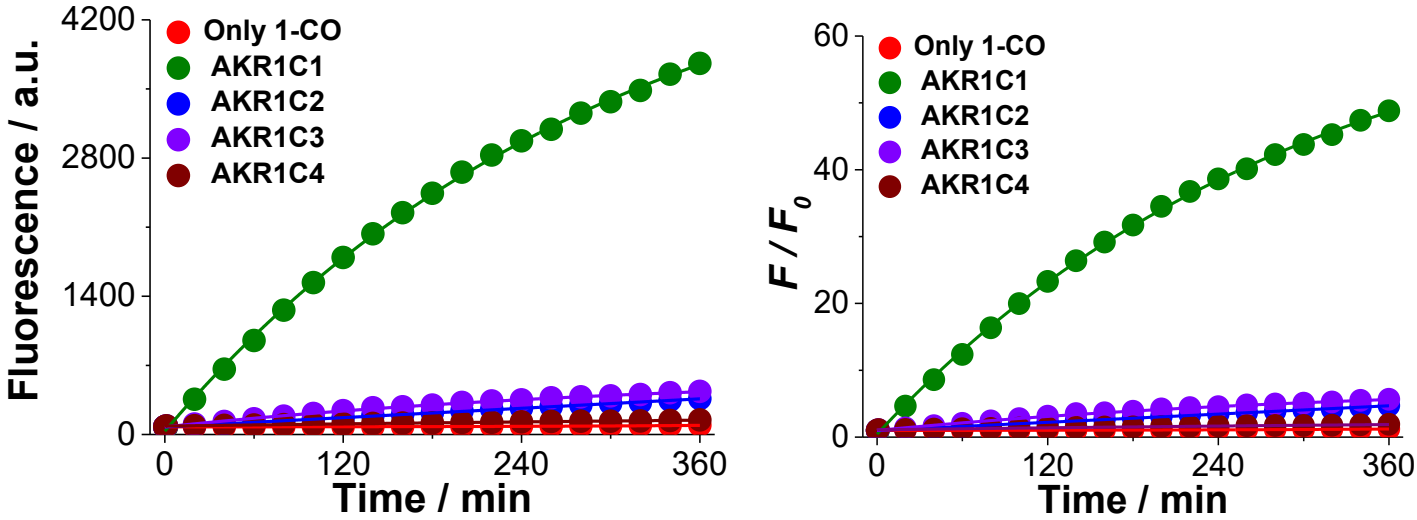

Figure S19. Time-dependent fluorescence intensity changes of **1-CO** (4 μM) in the presence of AKR1C family isoforms (AKR1C1, AKR1C2, AKR1C3, AKR1C4; 100 nM each). All measurements were performed in phosphate buffer (10 mM, pH 7.4, 50 μM NADPH, 1% DMSO) at 37 °C. λ_{ex} = 470 nm, λ_{em} = 524 nm.

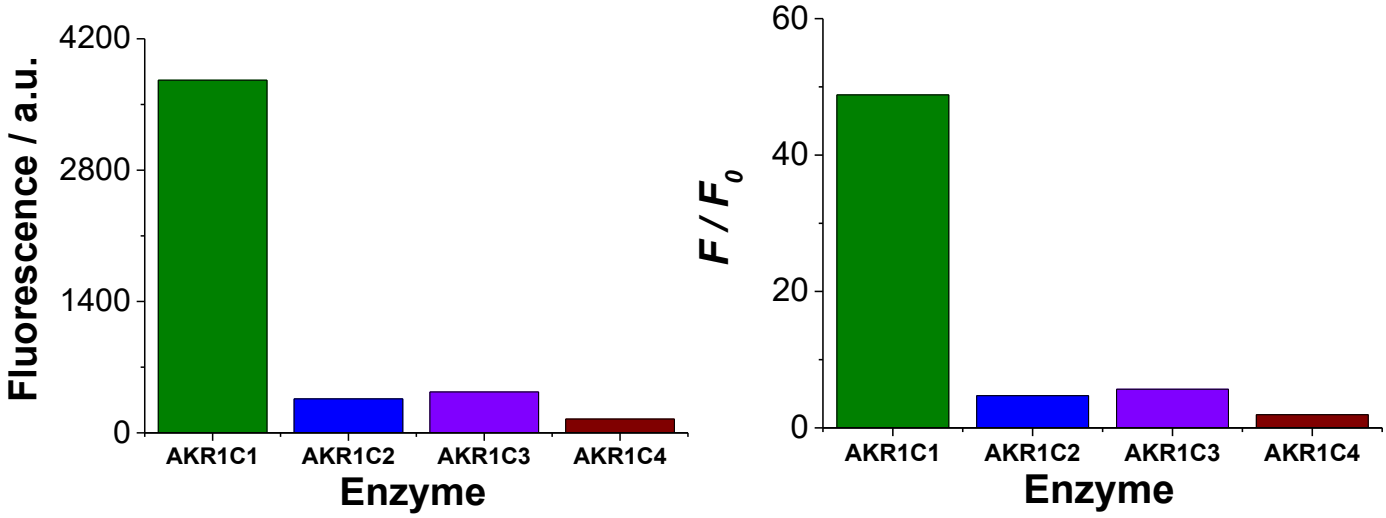

Figure S20. Comparative fluorescence turn-on responses of **1-CO** (4 μM) toward AKR1C isoforms (100 nM each) after 6 h incubation. All measurements were performed in phosphate buffer (10 mM, pH 7.4, 50 μM NADPH, 1% DMSO) at 37 °C. λ_{ex} = 470 nm, λ_{em} = 524 nm.

*Time-dependent fluorescence response of **1-CO** with AKR1C1/NADPH over 24 hours*

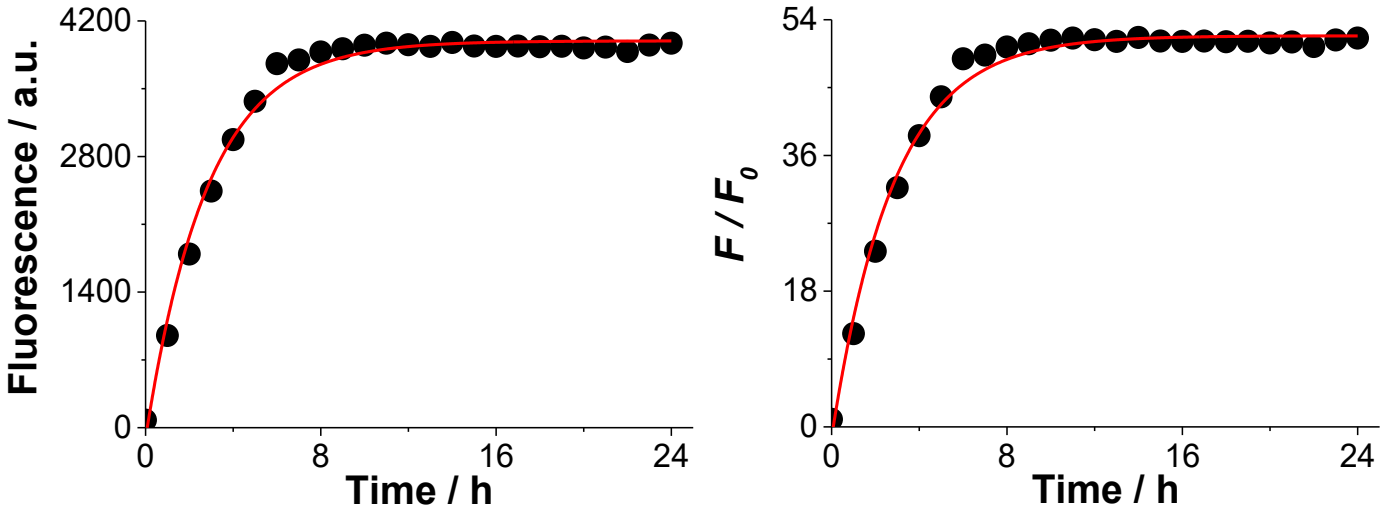

Figure S21. Time-dependent fluorescence intensity changes of **1-CO** (4 μM) upon incubation with AKR1C1 (100 nM) in phosphate buffer (10 mM, pH 7.4, 1% DMSO, 50 μM NADPH) at 37 °C. Spectra were obtained every 1 hour over 24 h. λ_{ex} = 470 nm, λ_{em} = 524 nm.

*Confirmation of enzymatic reaction product of **1-CO** with AKR1C1/NADPH by ESI-MS*

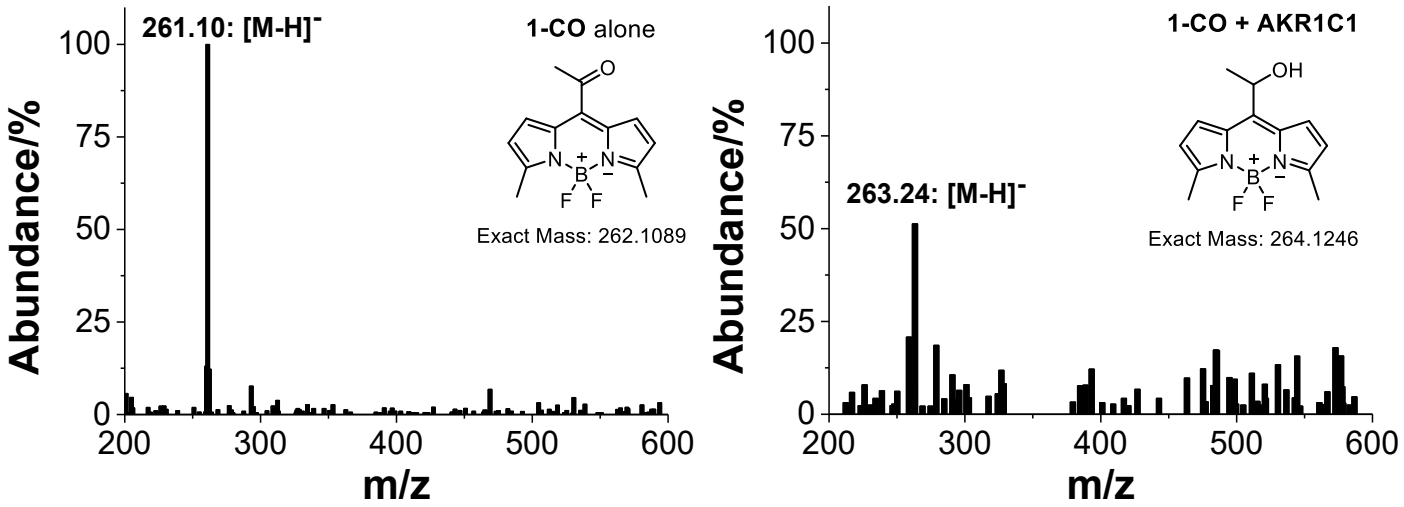

Figure S22. ESI-MS spectra (negative mode) of **1-CO** (10 μM) in phosphate buffer (10 mM, pH 7.4, 50 μM NADPH, 1% DMSO) before (left) and after (right) treatment with AKR1C1 (100 nM) for 6 h at 37 °C. The samples were analyzed isocratically at a ratio of solvent A (water) 50% and solvent B (acetonitrile) 50% for 20 min, with a flow rate of 0.3 mL/min. (left) ESI-MS spectrum of **1-CO** alone showed the peak at *m*/*z* 261.10, which corresponds to $[M-H]^-$ for **1-CO**. (right) ESI-MS spectrum of **1-CO** after treatment with AKR1C1 (100 nM) for 6 h showed the peak at *m*/*z* 263.24, which corresponds to $[M-H]^-$ for the reduction product, **1-OH**.

(b) Enzymatic sensing response of 2-CO and isoform selectivity

*Time-dependent emission spectrum of **2-CO** without and with NADPH*

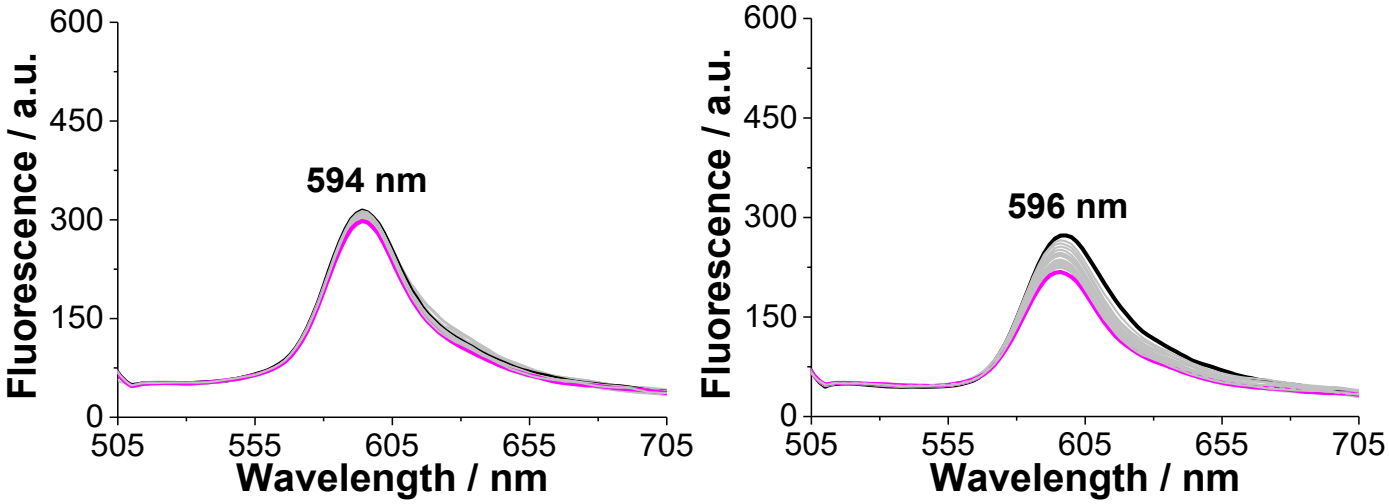

Figure S23. Time-dependent emission spectra of **2-CO** (4 μM) in the absence (left) and presence (right) of NADPH (50 μM). All measurements were performed in phosphate buffer (10 mM, pH 7.4, 1% DMSO) at 37 °C. Spectra were obtained every 20 min over 6 h (λ_{ex} = 470 nm). Black and pink lines indicate the spectra of **2-CO** before and after 6 h incubation, respectively.

*Time-dependent emission spectrum of **2-CO** with AKR1C1/NADPH and AKR1C2/ NADPH*

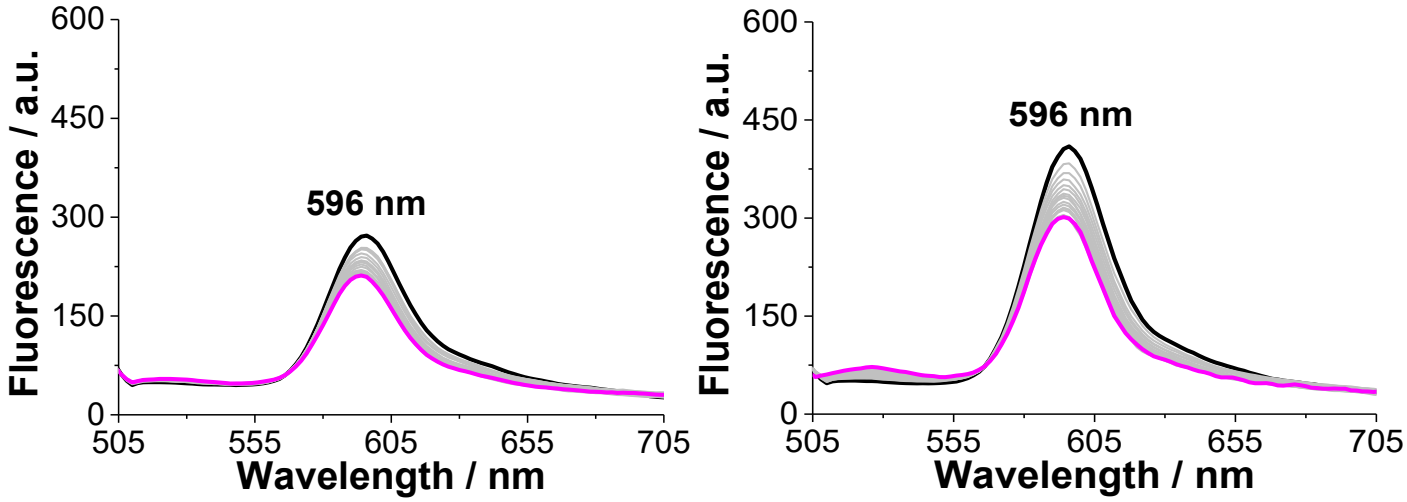

Figure S24. Time-dependent emission spectra of **2-CO** (4 μM) upon incubation with AKR1C1 (100 nM, left) and AKR1C2 (100 nM, right) in phosphate buffer (10 mM, pH 7.4, 1% DMSO, 50 μM NADPH) at 37 °C. Spectra were obtained every 20 min over 6 h (λ_{ex} = 470 nm). Black and pink lines indicate the spectra of **2-CO** before and after 6 h incubation with AKR1C1 (left) and AKR1C2 (right), respectively.

*Time-dependent emission spectrum of **2-CO** with AKR1C3/NADPH and AKR1C4/ NADPH*

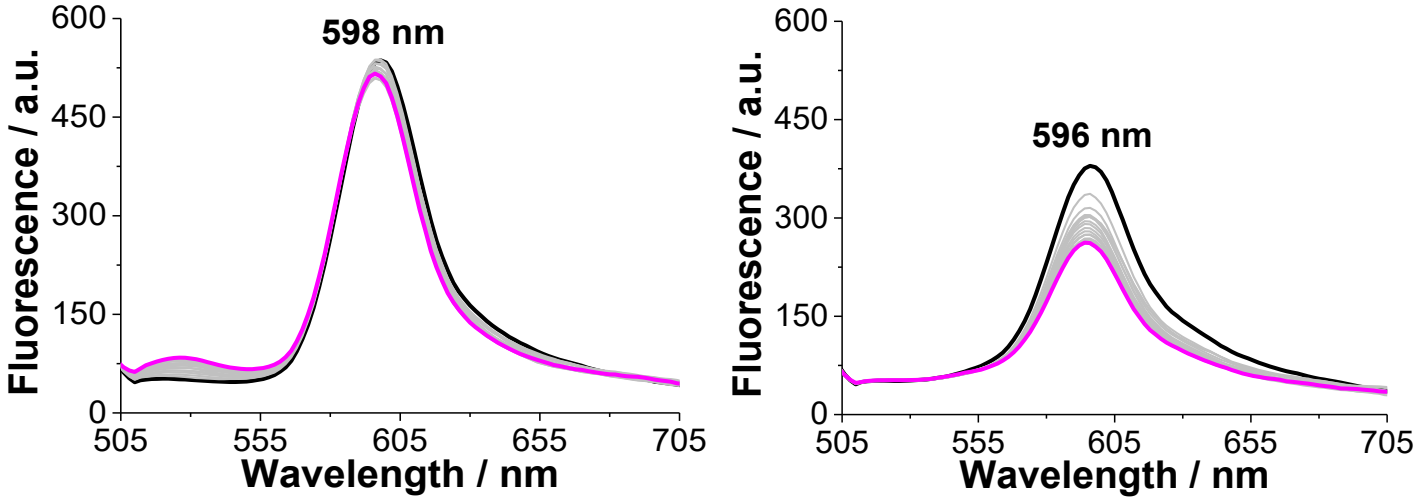

Figure S25. Time-dependent fluorescence response of **2-CO** (4 μM) upon addition of AKR1C3 (100 nM, left) and AKR1C4 (100 nM, right) in phosphate buffer (10 mM, pH 7.4, 1% DMSO, 50 μM NADPH) at 37 °C over 6 h. Black and pink lines indicate the spectra of **2-CO** before and after 6 h incubation with AKR1C3 (left) and AKR1C4 (right), respectively.

*Comparative fluorescence turn-on responses of **2-CO** toward AKR1C isoforms*

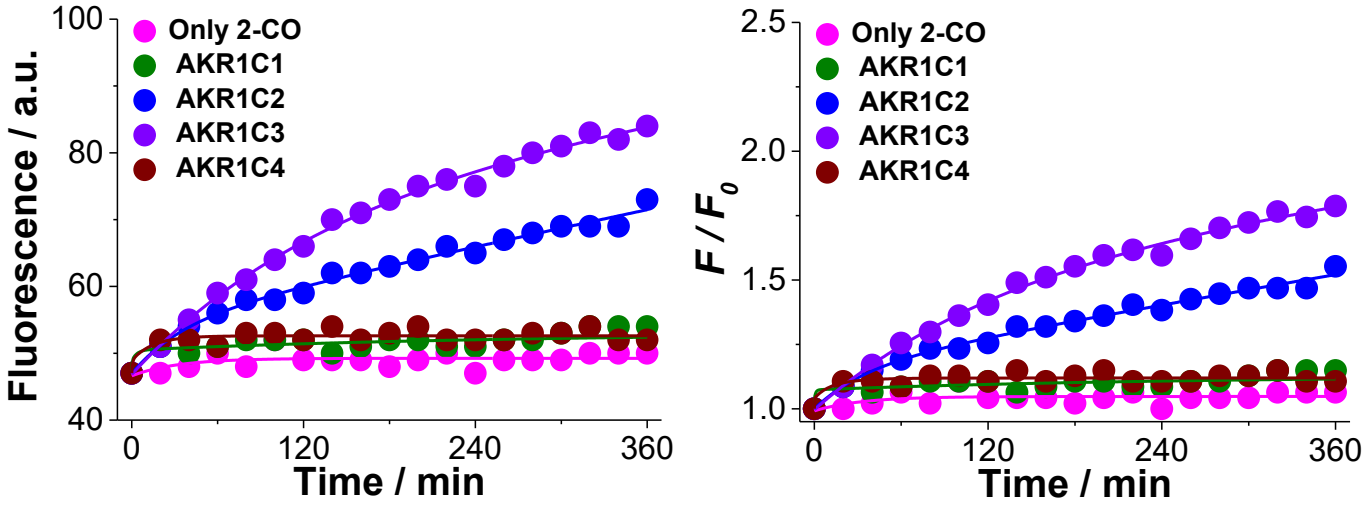

Figure S26. Time-dependent fluorescence intensity changes (F/F_0) of **2-CO** (4 μM) in the presence of AKR1C family isoforms (AKR1C1, AKR1C2, AKR1C3, AKR1C4; 100 nM each). All measurements were performed in phosphate buffer (10 mM, pH 7.4, 50 μM NADPH, 1% DMSO) at 37 °C. λ_{ex} = 470 nm, λ_{em} = 526 nm.

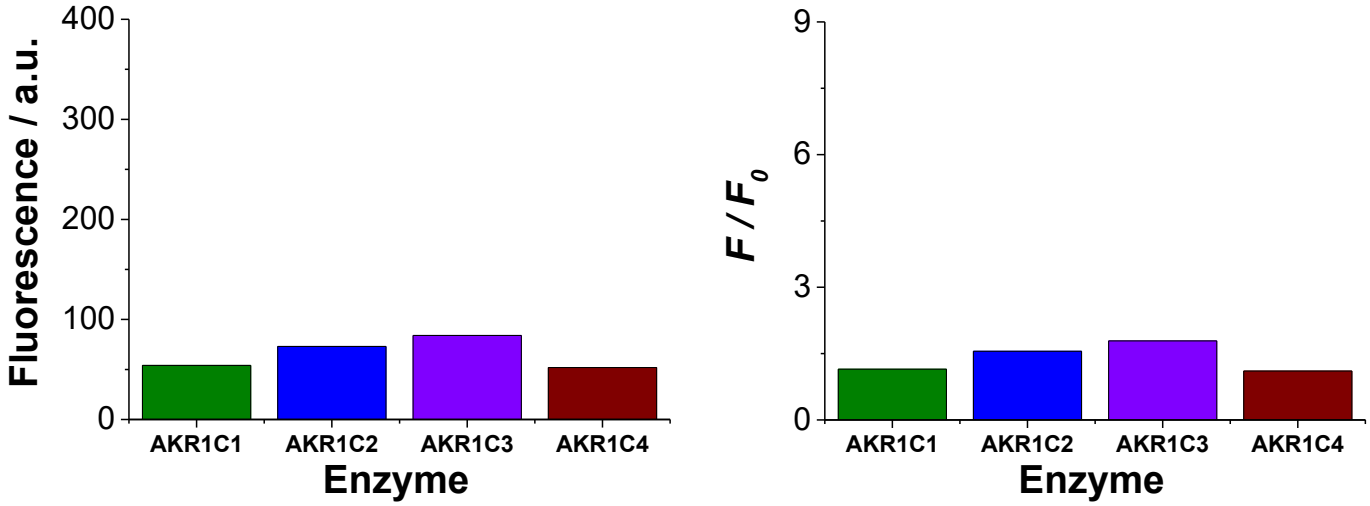

Figure S27. Comparative fluorescence turn-on responses of **2-CO** (4 μM) toward AKR1C isoforms (100 nM each) after 6 h incubation. All measurements were performed in phosphate buffer (10 mM, pH 7.4, 50 μM NADPH, 1% DMSO) at 37 °C. λ_{ex} = 470 nm, λ_{em} = 526 nm.

5. Photostability Studies

We investigated the photostability of **1-CO** and **2-CO** in water (DMSO 5%) at 25 °C. The photooxidation studies were performed by continuous irradiation using a 150 W steady-state Xenon lamp as the irradiation source under aerobic conditions for 60 minuites. The photoinduced degradation was quantified by monitoring the decrease of fluorescence intensity as a function of elapsed photolysis time.

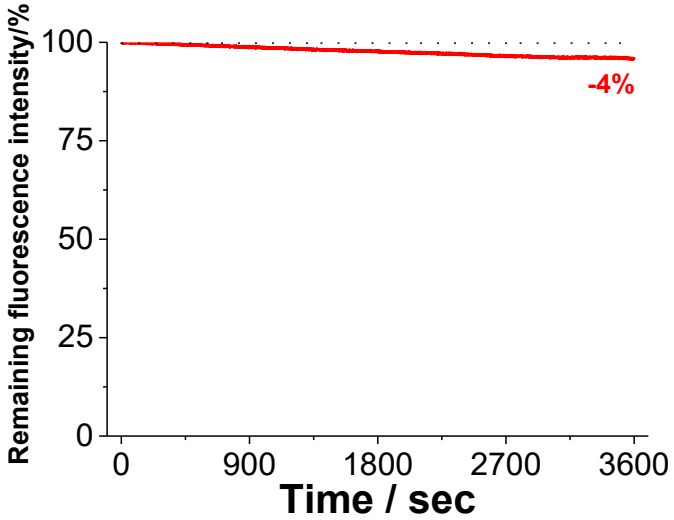

Figure S28. Photostability of **1-CO** in water (DMSO 5%) at 25 °C. The remaining fluorescence emission intensities of **1-CO** as a function of irradiation time. Irradiated at 500 nm. Fluorescence intensity was measured at 623 nm. [**1-CO**] = 10 μM.

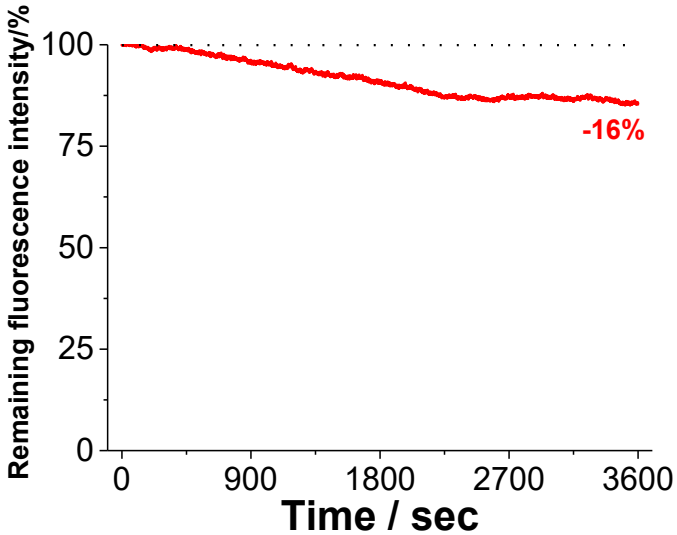

Figure S29. Photostability of **2-CO** in water (DMSO 5%) at 25 °C. The remaining fluorescence emission intensities of **2-CO** as a function of irradiation time. Irradiated at 500 nm. Fluorescence intensity was measured at 605 nm. [**2-CO**] = 10 μM.

6. Interference Studies

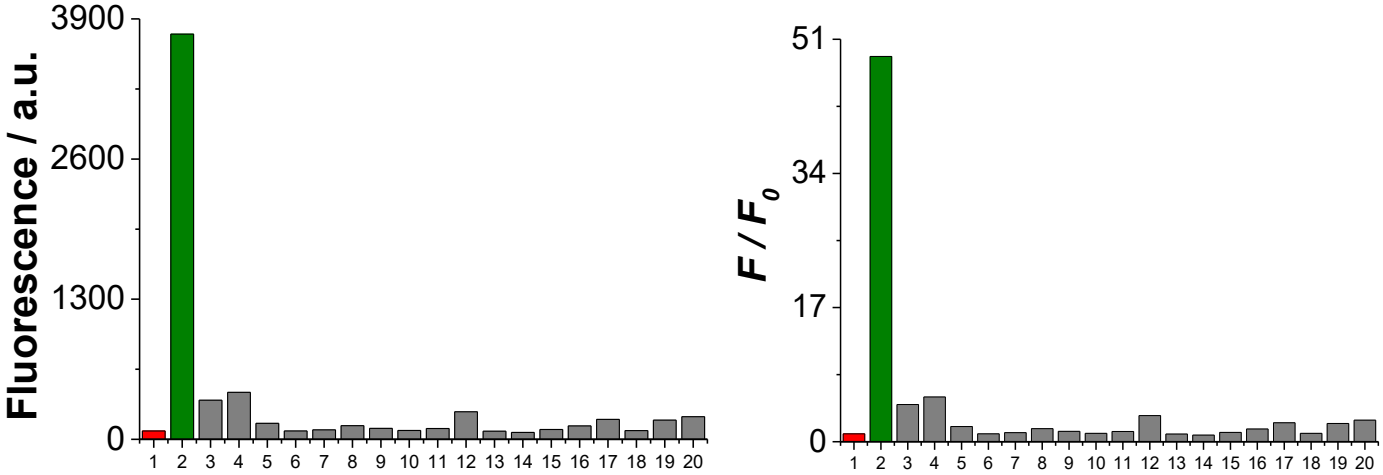

Figure S30. Relative fluorescence turn-on responses of **1-CO** to various biologically relevant species. Bars represent relative fluorescence intensity at 524 nm of **1-CO** (4 μM) in the presence of various species: (1) **1-CO** only (control), (2) AKR1C1 (100 nM), (3) AKR1C2 (100 nM), (4) AKR1C3 (100 nM), (5) AKR1C4 (100 nM), (6) trypsin (1 mg/mL), (7) lipase (1 mg/mL), (8) esterase (1 mg/mL), (9) BSA (1 mg/mL), (10) glucose (1 mg/mL), 11) L-glycine (1 mg/mL), (12) L-cysteine (1 mg/mL), (13) GSH (1 mg/mL), (14) homocysteine (1 mg/mL), (15) L-histidine (1 mg/mL), (16) L-lysine (1 mg/mL), (17) L-tryptophan (1 mg/mL), (18) NaOCl (200 μM), (19) ·OH (200 μM), (20) H_2O_2 (200 μM). All data were obtained in phosphate buffer (10 mM, pH 7.4, 50 μM NADPH, 1% DMSO) at 37 °C. λ_{ex} = 470 nm, λ_{em} = 524 nm. Incubation time = 6 h. F and F_0 correspond to fluorescence intensity of **1-CO** in the presence and absence of each analyte, respectively.

7. Enzyme Kintetics

To determine the kinetic constants, **1-CO** at a series of the final concentrations (0.5–6 μM) was reduced by AKR1C1 in the assay buffer solution (10 mM phosphate buffer, pH 7.4, 50 μM NADPH) at 37 °C. The reaction was monitored by measuring fluorescence intensities at 524 nm for product **1-OH** (excited at 470 nm). The initial velocity was calculated from the slope of the each progress curve.

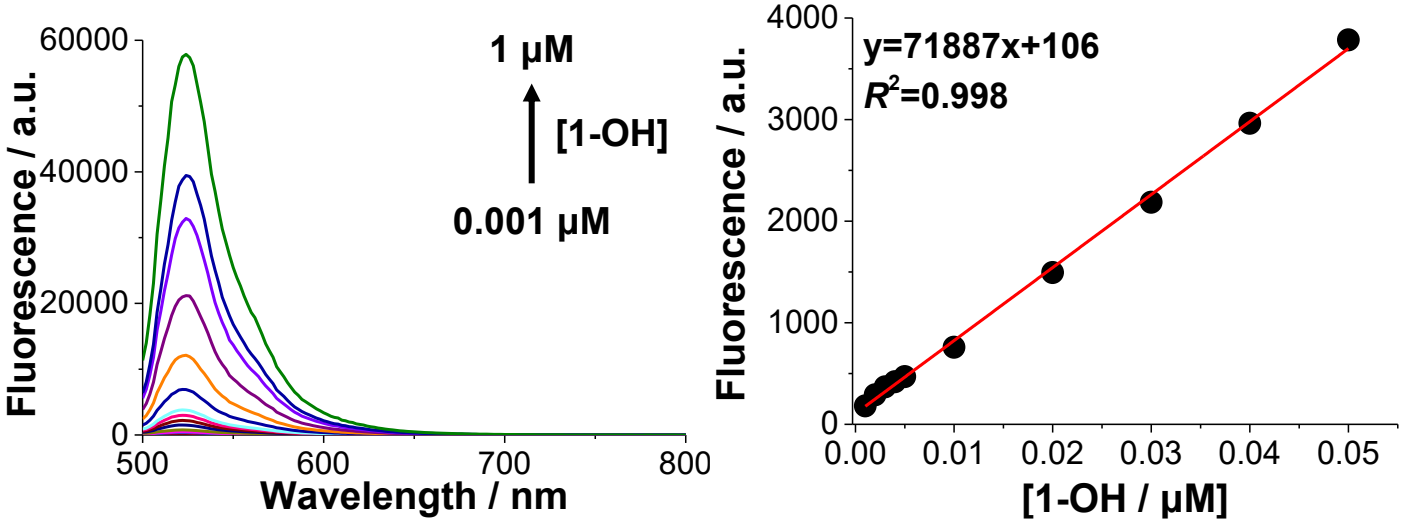

Figure S31. (left) Fluorescence emission spectra of **1-OH** at different concentrations (0.001−1 μM) in phosphate buffer (10 mM, pH 7.4) containing 1% DMSO as a cosolvent at 37 °C. Excited at 470 nm. (right) A linear relationship between fluorescence intensity at 524 nm and amounts of **1-OH** (0–0.05 μM).

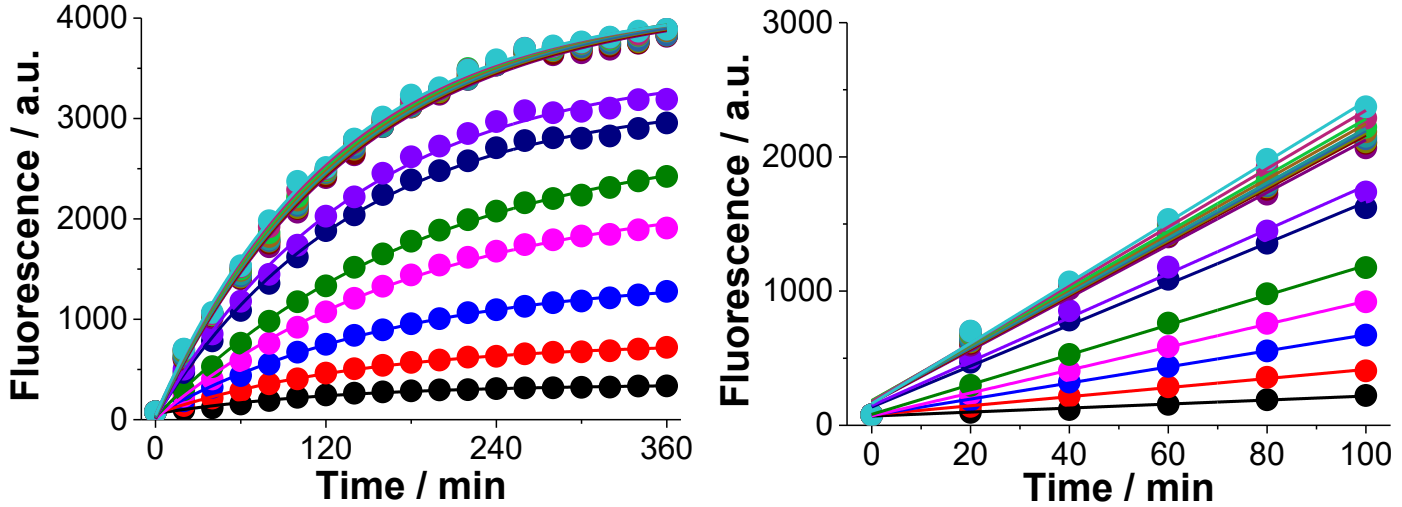

Figure S32. Time-dependent changes of fluorescence intensity ratio of **1-CO** (0.5–6 μM) upon incubation with AKR1C1 (100 nM). The emission spectra were obtained every 20 min (0–360 min) after the addition of AKR1C1 to **1-CO** (4 μM) and NADPH (50 μM) in phosphate buffer (10 mM, pH 7.4) at 37 °C. Fluorescence intensity at 524 nm was recorded with excitation at 470 nm.

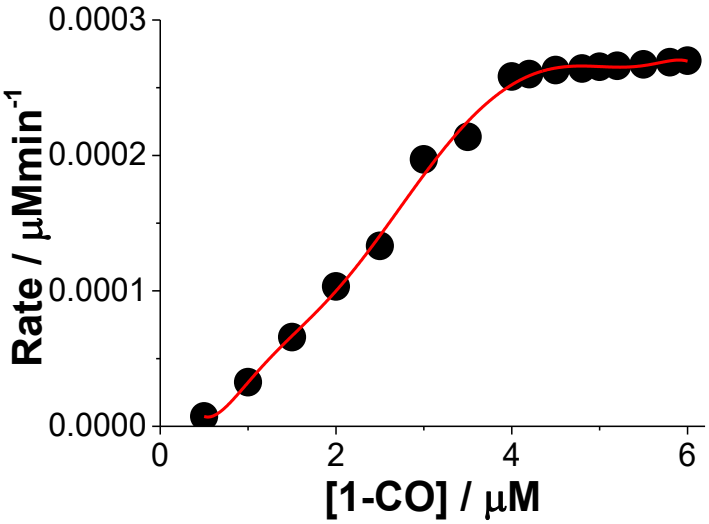

Figure S33. A plot of the initial velocity v_0 of the reaction of **1-CO** (0.5–6 μM) with NADPH (50 μM) and AKR1C1 (100 nM) versus concentration of **1-CO**.

Table S3. Summary of kinetic parameters

Substrates	K_M (μM)	k_{cat} (min^{-1})	k_{cat}/K_M (min^{-1} mM^{-1})
1-CO	2.43	2.70×10^{-3}	1.11
5α-DHT[4] 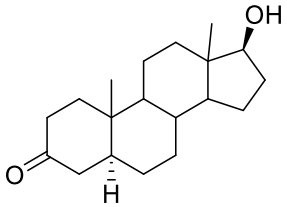	80.6 ± 28.8	0.66	8
progesterone[4] 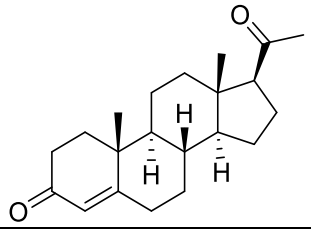	2.65 ± 0.66	0.29	109

8. Inhibition Assay

For inhibition assay of **1-CO** activity, final concentration of **1-CO**, NADPH and AKR1C1 were fixed to 4 μM, 50 μM and 100 nM, respectively. AKR1C1 inhibitor, 3-bromo-5-phenylsalicylic acid (5-PBSA) was dissolved in phosphate buffer (10 mM, pH 7.4) to obtain a stock solution of 200 μM and the stock solution was diluted with phosphate buffer (10 mM, pH 7.4) to achieve concentrations ranging from 0.0001 μM to 100 μM. To 197 μL of working solution of phosphate buffer (10 mM, pH 7.4, 50 μM NADPH, 100 nM AKR1C1) was added to 2 μL of a solution of inhibitor, the mixed solutions were incubated at 37 ˚C for 30 min to inhibit enzyme activity. To the inhibitor-treated working solution was added 2 μL of **1-CO** (4 μM) dissolved in DMSO. Fluorescence intensities at 524 nm was recorded every 5 min for 3 hours at 37 ˚C.

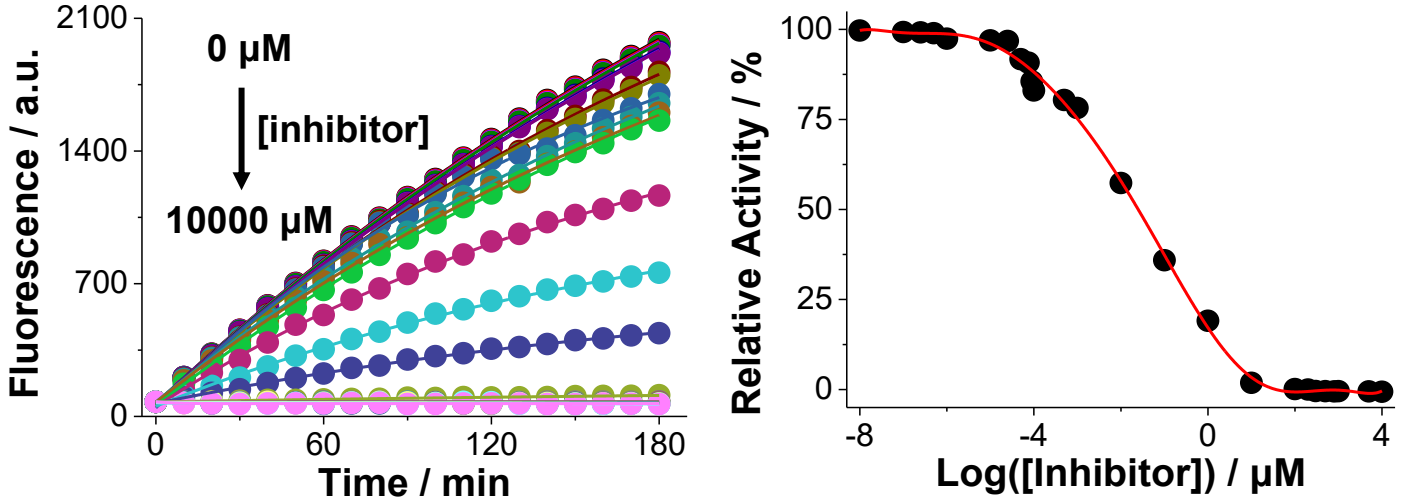

Figure S34. Inhibition assay of AKR1C1 activity using **1-CO** in 10 mM phosphate buffer (10 mM, pH 7.4) at 37 °C. (left) Kinetic profiles of **1-CO** (4 μM) after the addition of a solution of **1-CO** to each NADPH and A KR1C1 solution, which was pretreated with 3-bromo-5-phenylsalicylic acid (5-PBSA) at different concentrations (from top to bottom: 0, 0.00000001, 0.0000001, 0.00000025, 0.0000005, 0.000001, 0.00001, 0.000025, 0.00005, 0.000075, 0.00009, 0.0001, 0.0005, 0.001, 0.01, 0.1, 1, 10, 100, 200, 300, 500, 800, 1000, 10000 μM) for 180 min at 37 °C. The emission spectra were obtained every 3 min (0-180 mn) after each treatment, and fluorescence intensities at 524 nm was recorded. Excited at 470 nm. (right) Relative activity of AKR1C1 versus concentration of 3-bromo-5-phenylsalicylic acid (5-PBSA) (0–10000 μM) at 180 min time point. IC_{50} was determined to be 24.6± 0.5 nM. [**1-CO**] = 4 μM. [NADPH] = 50 μM. [AKR1C1] = 100 nM.

Table S4. Reported fluorogenic probes for detection of AKR1C activity

Probes	Mechanism	Signal change	Isoform selectivity	Reference
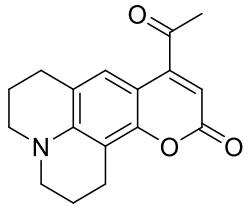	Intramolecular charge transfer (ICT) modulation	25-fold increase after 12 h incubation	focus on AKR1C3 (no selectivity data)	*J. Am. Chem. Soc.,* 2004, **126**, 2282
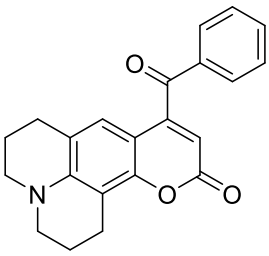	Intramolecular charge transfer (ICT) modulation	Upto 300-fold (two-photon excitation)	focus on AKR1C3 (no selectivity data)	*J. Phys. Chem. C,* 2007, **111**, 8872
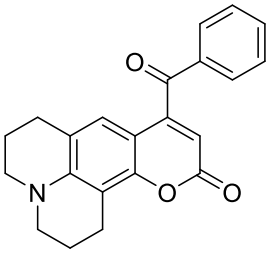	Intramolecular charge transfer (ICT) modulation	20% conversion after 24 h in mock-transfected cells vs. complete conversion after 4 h in AKR1C2-transfected cells	focus on AKR1C2 in intact cells (no selectivity data)	*Proc. Natl. Acad. Sci. U. S. A.,* 2006, **103**, 13304
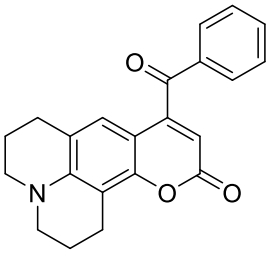	Intramolecular charge transfer (ICT) modulation	3-4 fold increase in fluorescence with ARE inducers in cells	AKR1C3 or AKR1C2	*J. Am. Chem. Soc.,* 2008, **130**, 14123

9. Molecular Docking Studies of Probes for AKR1C1

Molecular docking calculations were performed using Molegro Virtual Docker (MVD, version 6.0).[5] The crystal structure of AKR1C1 (PDB code: 3C3U) was obtained from the Protein Data Bank (PDB). The 3D structures of the ligands were modeled with PerkinElmer Chem3D version 15.0.[6] The binding site was automatically defined as a 15 Å radius centered around 3,5-dichlorosalicylic acid in complex, as identified by MVD. Docking simulations were executed using MVD's docking wizard with standard parameters, revealing distinct binding modes for the two probes (Fig. S32). Probe **1-CO** exhibited favorable interactions within the AKR1C1 active site, including hydrogen bonding with Tyr24, electrostatic interactions with His117, and extensive hydrophobic contacts with surrounding residues. The binding pose also showed steric interactions with Tyr55 and His117, yielding a MolDock score of −73.92. In contrast, **2-CO** displayed a markedly different binding mode with no hydrogen bonding, two electrostatic interactions with His222, and hydrophobic contacts with surrounding residues. However, unfavorable steric clashes with Tyr24, His222, and Trp227 resulted in a less favorable MolDock score of −56.69. The more favorable docking score for **1-CO** is consistent with its superior enzymatic performance and suggests optimal geometric complementarity within the AKR1C1 active site.

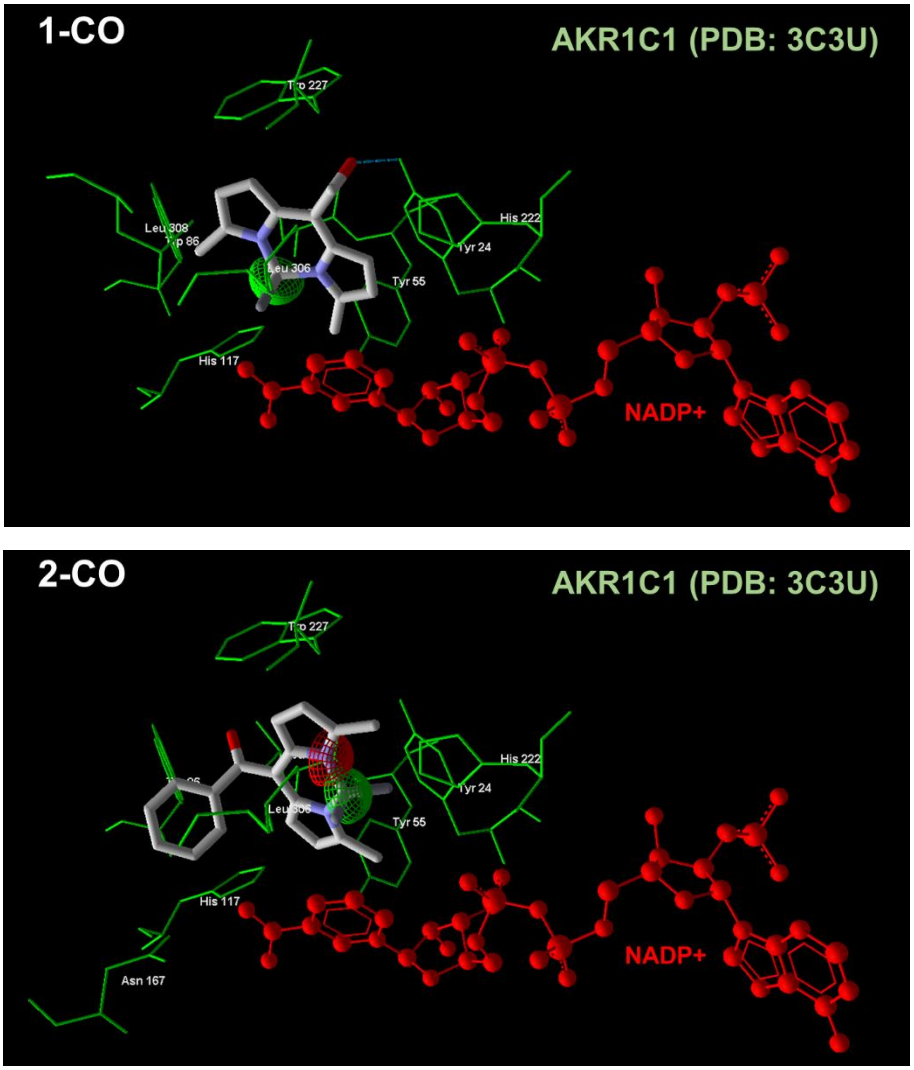

Figure S35. Molecular docking poses of **1-CO** (top) and **2-CO** (bottom) in the AKR1C1 active site (PDB: 3C3U). Each probe (shown in gray stick representation) was positioned within the AKR1C1 binding pocket alongside the $NADP^+$ cofactor (red). Key residues were shown as green-colored thin sticks. Hydrogen bonds between the probe and key residues were indicated by blue dashed lines. Electrostatic interaction between the probe and key residues residue was indicated by red-lined (negative) or green (positive) cap.

10. Cell Studies

Cell viability assay

Human cervical carcinoma HeLa cells (ATCC CCL-2) and human lung adenocarcinoma A549 cells (ATCC CCL-185) were obtained from American Type Culture Collection (ATCC, Manassas, VA) and maintained in Dulbecco's modified Eagle medium (DMEM; GenDEPOT, Barker, TX, USA) supplemented with 10% fetal bovine serum (FBS; GenDEPOT, Barker, TX, USA) and 1% antibiotic–antimycotic (GenDEPOT, Barker, TX, USA) and maintained in a humidified environment with 5% CO_2 at 37 °C.

To measure the cytotoxicity of **1-CO** compound, a 3-(4,5-dimethylthiazol-2-yl)-2,5-diphenyltetrazolium bromide (MTT) assay was performed. Briefly, a density of 1×10^4 cells of HeLa or A549 cell lines in complete medium were seeded on each well of 96-well cell culture plates (SPL Life Science Co., Gyeonggi-do, Republic of Korea). After 24 h, the cells were treated with various concentrations of **1-CO** compound, consisting of 0.5, 1.0, 2.0, 4.0, and 8.0 μM, in cell culture medium for 24 h at 37 °C. Following the standard procedure, 100 μL of MTT (1 mg/mL) (Invitrogen, Waltham, Massachusetts, USA) was added to each well and incubated for three hours. The medium was then discarded, and the resulting formazan product was dissolved in 100 μL dimethyl sulfoxide (DMSO). Absorbance was read at 570 nm using a Mithras2 plate reader (Berthold Technologies, Bad Wildbad, Germany). The cell viability was calculated as a percentage relative to the control.

Intracellular localization

HeLa or A549 cells were seeded in confocal dishes (SPL Life Science Co., Gyeonggi-do, Republic of Korea) at a density of 2×10^5 cells per dish. To observe subcellular localization, the cells were incubated with 2 μM of **1-CO** for 6 h and 2 μM ER Tracker Blue-White (Molecular Probes, Eugene, OR, USA) for another 30 min, then imaged by using a TCS-SP8 confocal laser scanning microscope (Leica, Germany). The product of **1-CO** compound was excited at 488 nm, and emission in the range of 493–560 nm was measured. The blue fluorescence of live cells treated with commercial probe was collected at 410–490 nm after excitation at 405 nm.

Cellular fluorescence imaging

HeLa or A549 cells were seeded in confocal dishes (SPL Life Science Co., Gyeonggi-do, Republic of Korea) at a density of 2×10^5 cells per dish. After culturing overnight, the cells were treated with 2 μM of **1-CO** for different durations. To inhibit AKR1C1 activity, 10 μM of 5-PBSA was pretreated to the cells for 3 h before **1-CO** treatment. The fluorescence was imaged by a TCS-SP8 confocal laser scanning microscope (Leica, Germany) with the green fluorescence from product of **1-CO** (λ_{ex} = 488 nm, λ_{em} = 493–560 nm), and red fluorescence from **1-CO** (λ_{ex} = 561 nm, λ_{em} = 566–635 nm).

Western blot analysis

Total protein was extracted from HeLa or A549 cells with lysis buffer 1X RIPA (T&I, Gangwon, Republic of Korea). supplemented 0.02 tablet/mL protease inhibitor cocktail (#11697498001, Roche, Basel, Switzerland). The protein concentration was determined using a Bradford assay. Equal amounts of 20 μg protein were separated on 12% SDS-PAGE gels and transferred onto 0.45 μm Immobilon-P PVDF membrane (Merck KGaA, Darmstadt, Germany). After blocking with 5% skim milk in phosphate-buffered saline with 0.1% Tween 20 (PBST) for 1 h at room temperature, the membranes were incubated overnight at 4 °C with primary antibodies including rabbit anti AKR1C1 (GeneTex #GTX105620) and mouse anti-β-actin (Santa Cruz #47778) at dilution of 1:1000. Membranes were then washed and incubated with HRP-conjugated secondary antibodies of horse anti-mouse IgG (Cell signaling #7076) and goat anti-rabbit IgG (Cell signaling #7074) for 2 h at room temperature. Signals were detected using an enhanced chemiluminescence (ECL) solution (GenDEPOT, Barker, TX, USA) and an ImageQuant™ LAS 4000 biomolecular imager (GE Healthcare, Chicago, IL, USA).

Quantitation and statistical analysis

Intracellular colocalization was analyzed by ImageJ software. The significance of differences among multiple groups was determined by two-way analysis of variance (ANOVA). Differences between two groups were analyzed for significance using two-tailed Student's *t* tests. The *p* values are indicated as **p*<0.05, ***p*<0.01, ****p*<0.001, and *****p*<0.0001.

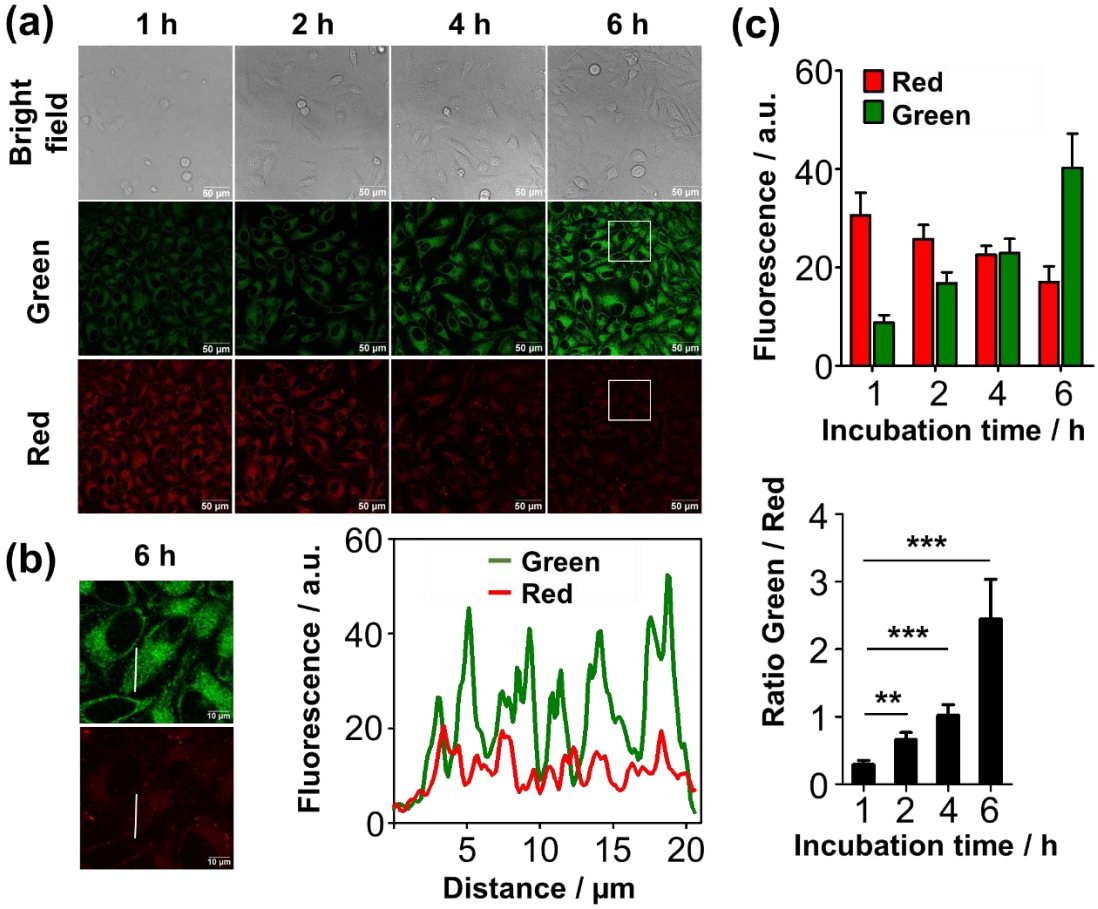

Figure S36. Real-time monitoring of endogenous AKR1C1 in living cells. (a) Confocal fluorescence images of HeLa cells treated with **1-CO** (2 μM, 6 h): bright-field, green (Ex/Em: 488/493–560 nm), and red (Ex/Em: 561/566–635 nm) channels. (b) Magnified images with line-scan profiles at 6 h. (c) Time-dependent fluorescence quantification and green/red ratios (mean ± SD, $n = 40$). **$p < 0.01$, ***$p < 0.001$. Scale bars: 50 μm (a), 10 μm (b).

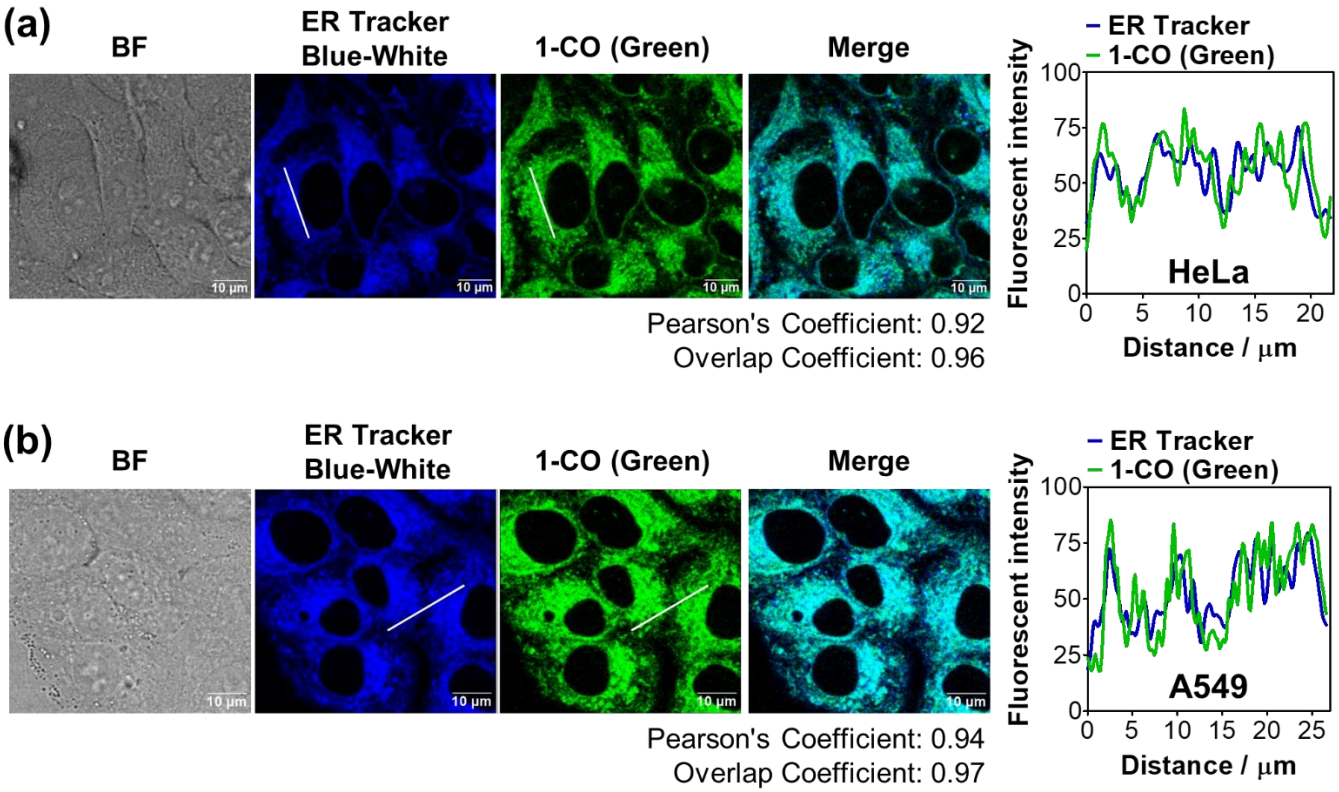

Figure S37. Subcellular localization of **1-CO** in living cells. Confocal fluorescence images of HeLa (a) and A549 (b) cells incubated with **1-CO** (2 μM, 6 h) and co-stained with ER-Tracker Blue-White (1 μM; λ_{ex} = 405 nm, λ_{em} = 410–490 nm). Enzyme-mediated activation of **1-CO** was detected in the green channel (λ_{ex} = 488 nm, λ_{em} = 493–560 nm). From left to right: bright-field (BF), ER-Tracker (blue), **1-CO** (green), and merged images. High Pearson's correlation coefficients (HeLa: 0.92; A549: 0.94) and overlap coefficients (HeLa: 0.96; A549: 0.97), along with line-scan profiles (right), confirm predominant localization of AKR1C1 activity within the endoplasmic reticulum. Scale bar = 10 μm.

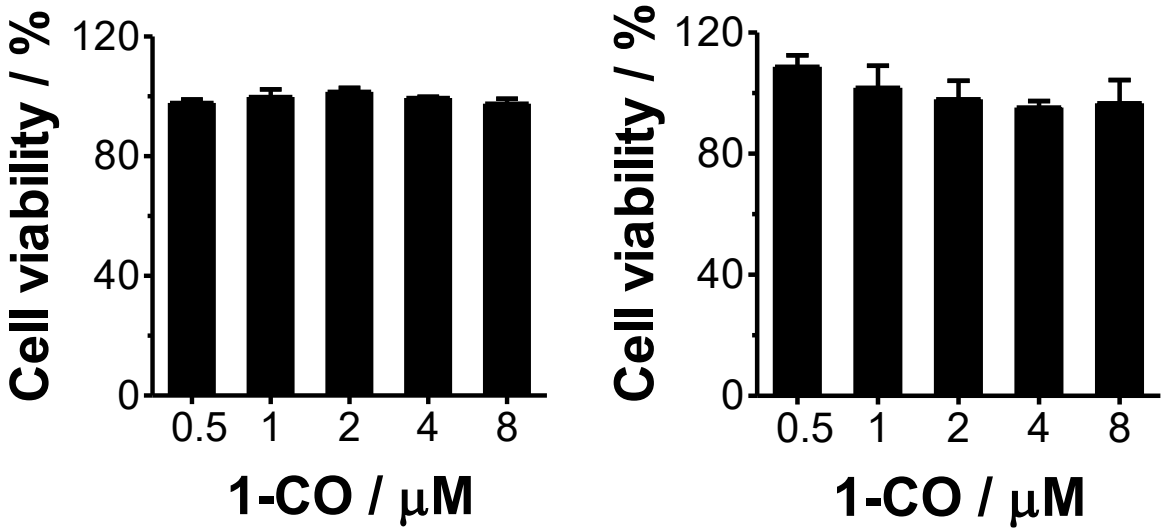

Figure S38. Cell viability of HeLa (left) and A549 (right) cells after 24 h treatment with **1-CO** at concentrations ranging from 0.5–8 μM, demonstrating excellent biocompatibility for live-cell applications. Data represent mean ± SD (n = 3).

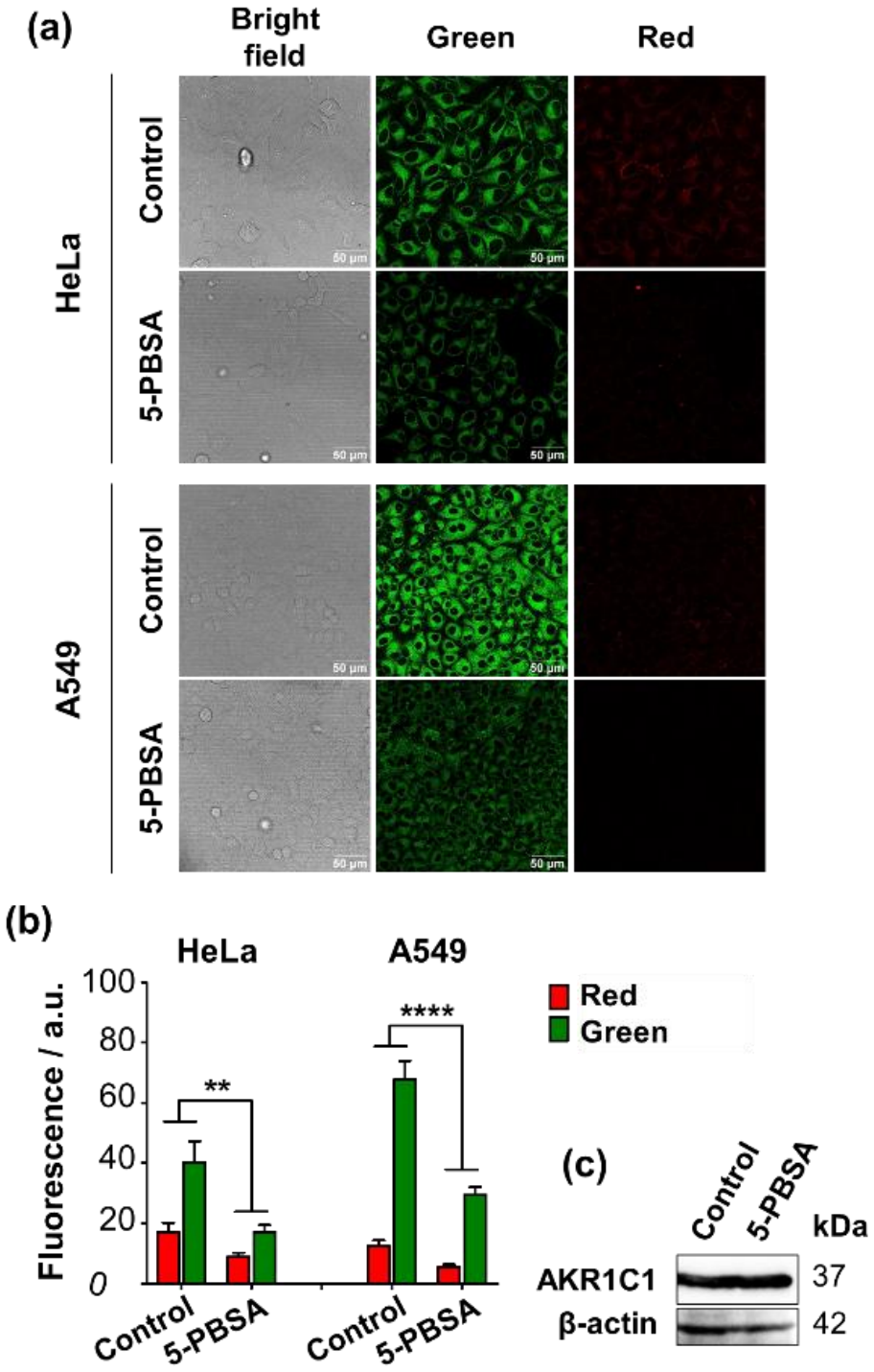

Figure S39. Inhibition of **1-CO** activation by AKR1C1 inhibitor 5-PBSA. (a) Confocal fluorescence images of HeLa and A549 cells with **1-CO** (2 μM, 6 h) without (control) and with 5-PBSA pretreatment (10 μM, 3 h): bright-field, green (Ex/Em: 488/493–560 nm), and red (Ex/Em: 561/566–635 nm) channels. Scale bar: 50 μm. (b) Fluorescence quantification (mean ± SD, $n = 40$; $^{**}p < 0.01$, $^{****}p < 0.0001$). (c) Western blot analysis of HeLa cells.

11. ^{1}H-NMR, ^{13}C-NMR, and HR-MS Spectra

^{1}H-NMR Spectrum of **1-OH** in $CDCl_3$ (500 MHz):

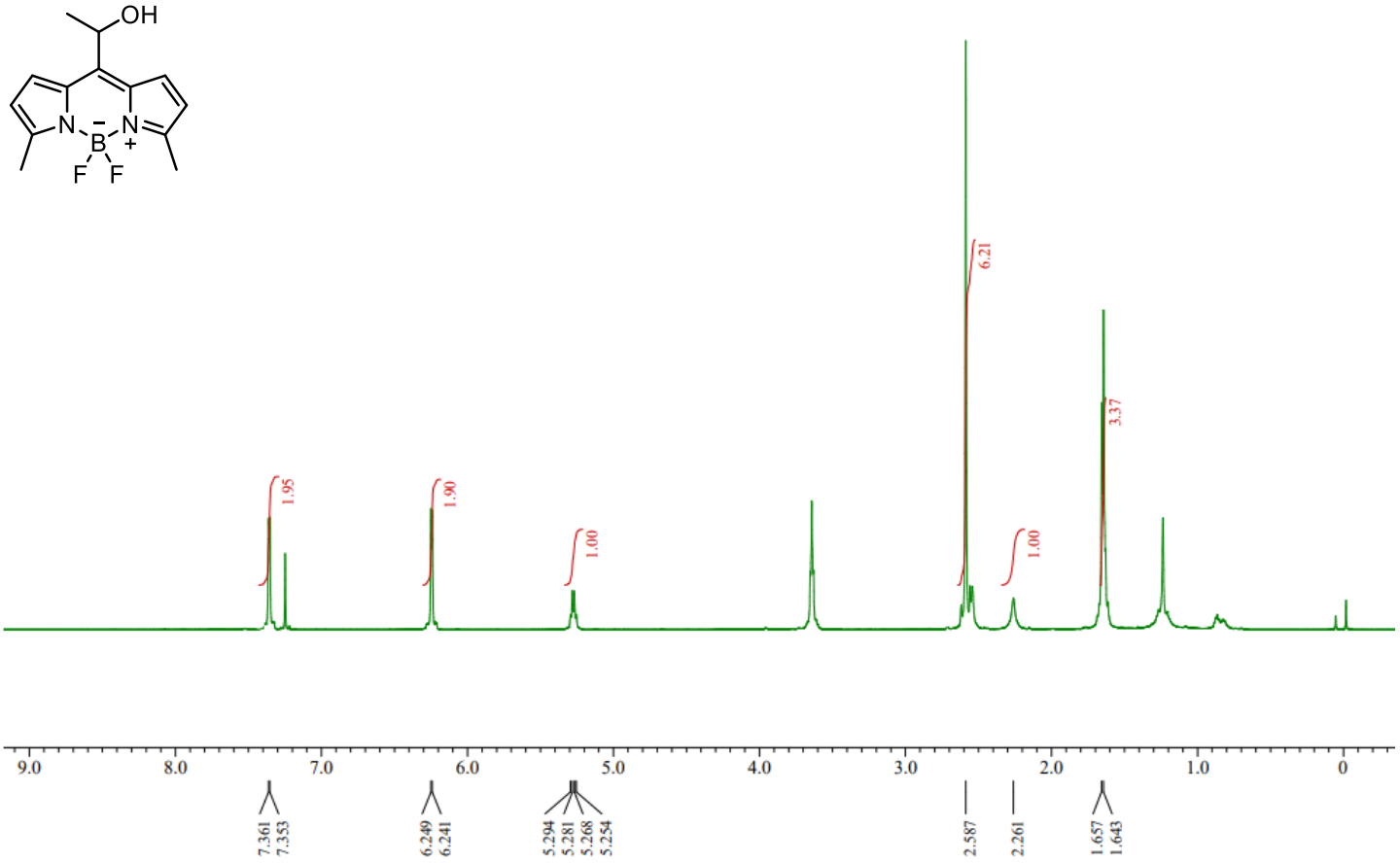

^{13}C-NMR Spectrum of **1-OH** in $CDCl_3$ (125 MHz):

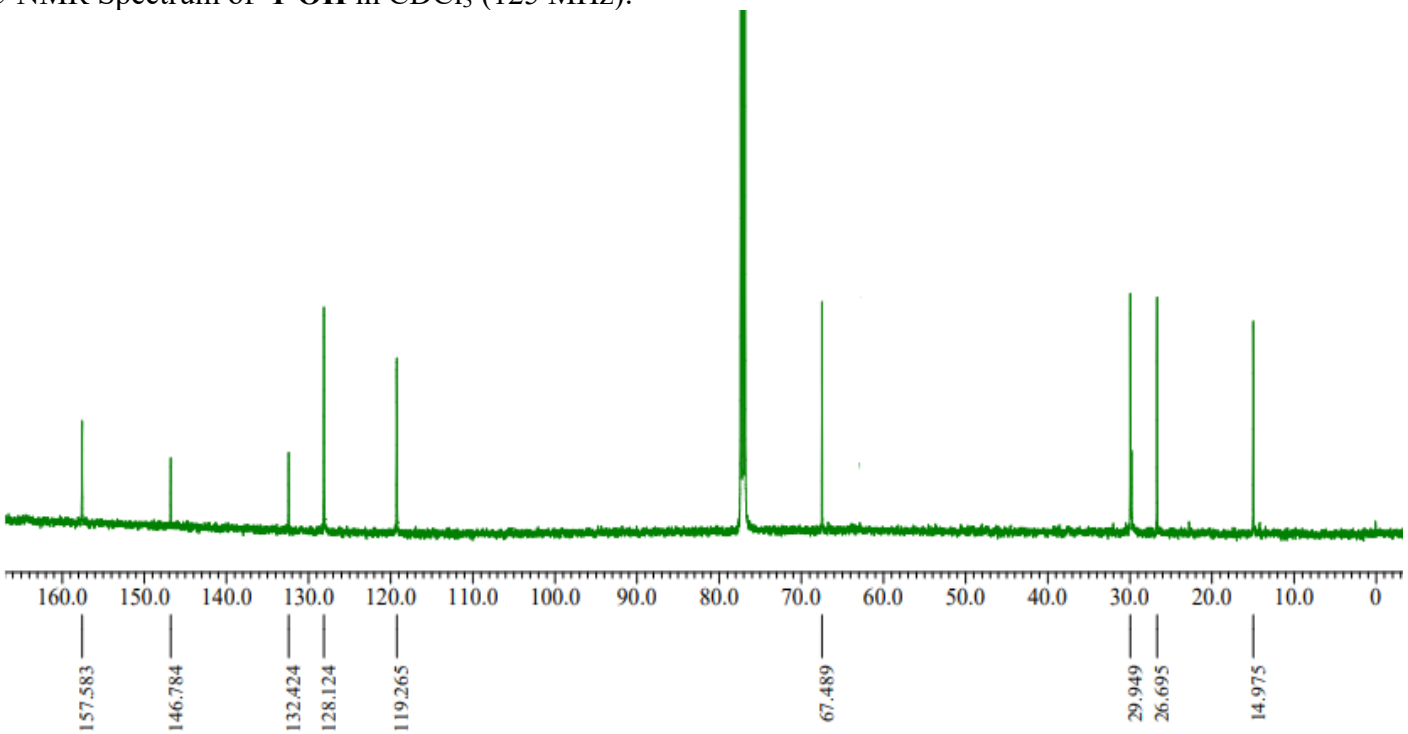

^{1}H-NMR Spectrum of **1-CO** in CD_2Cl_2 (500 MHz):

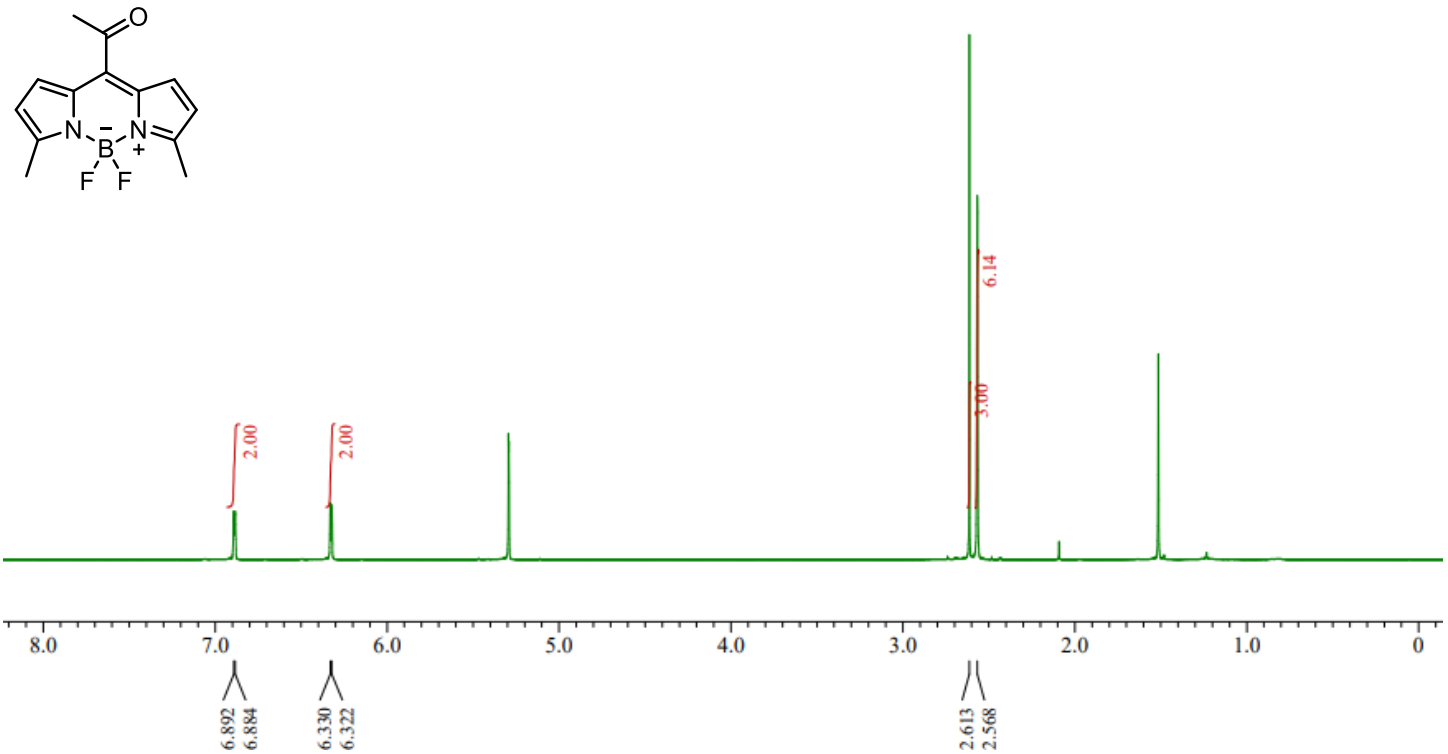

^{13}C-NMR Spectrum of **1-CO** in $CDCl_3$ (125 MHz):

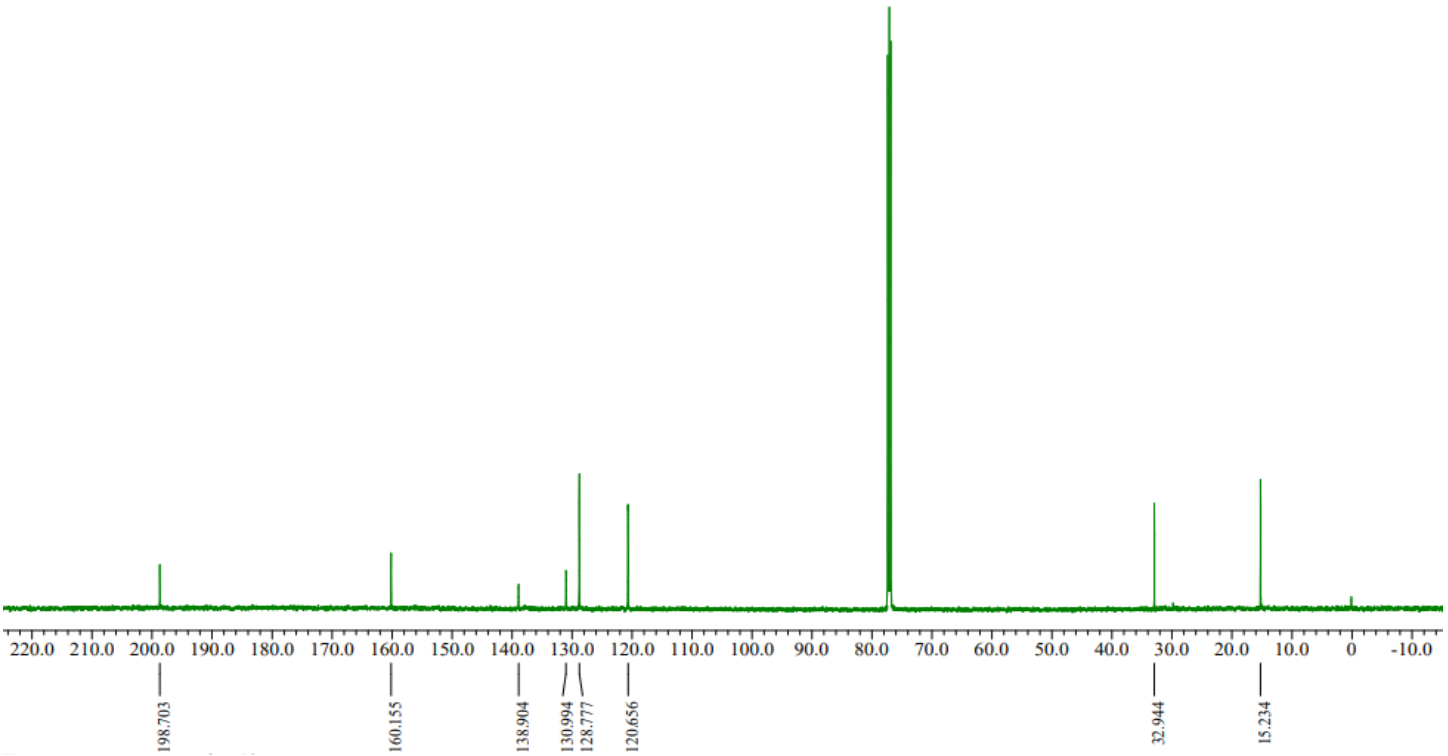

HR-MS Spectrum of **1-CO**:

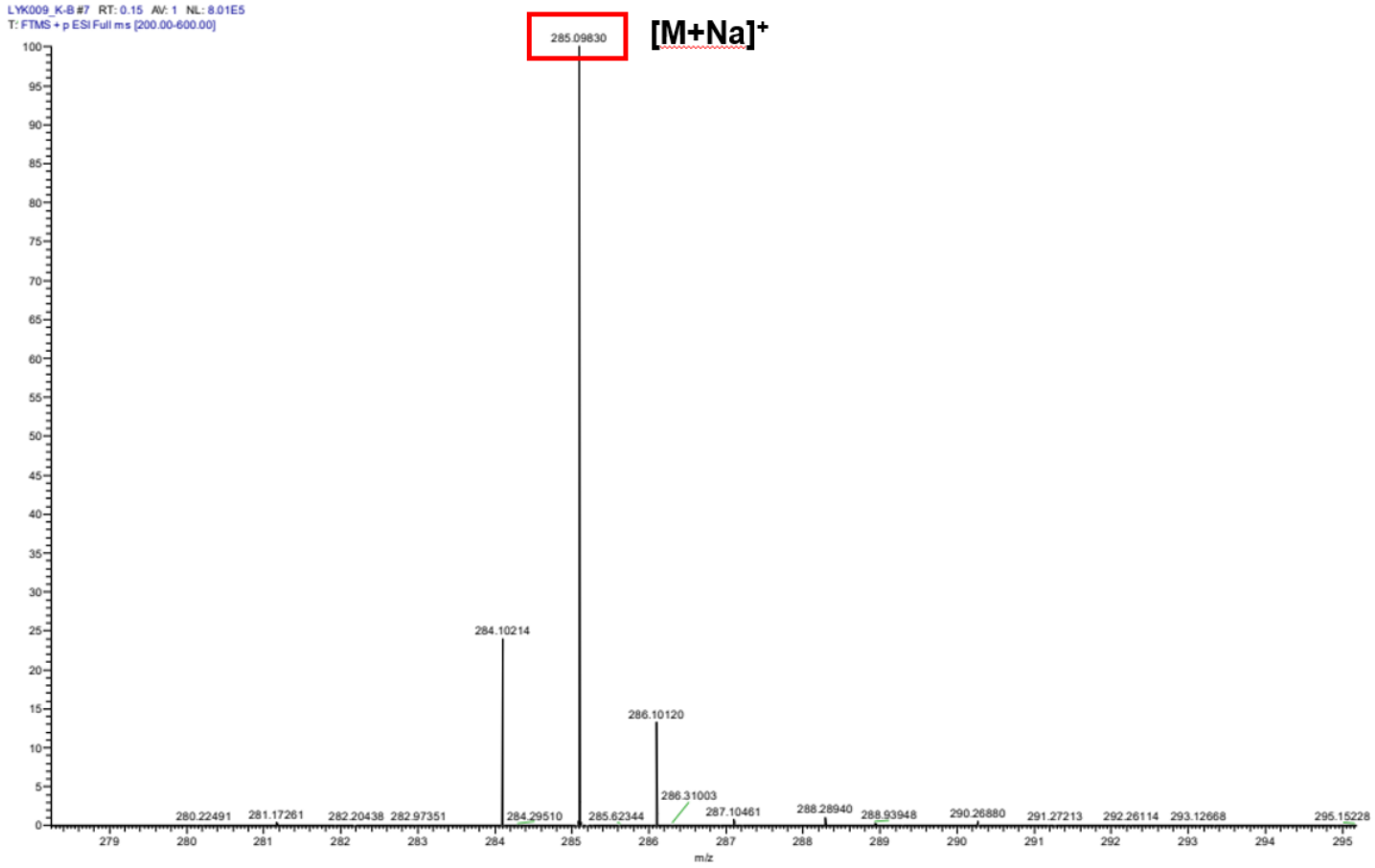

^{1}H-NMR Spectrum of **2-OH** in CD_2Cl_2 (500 MHz):

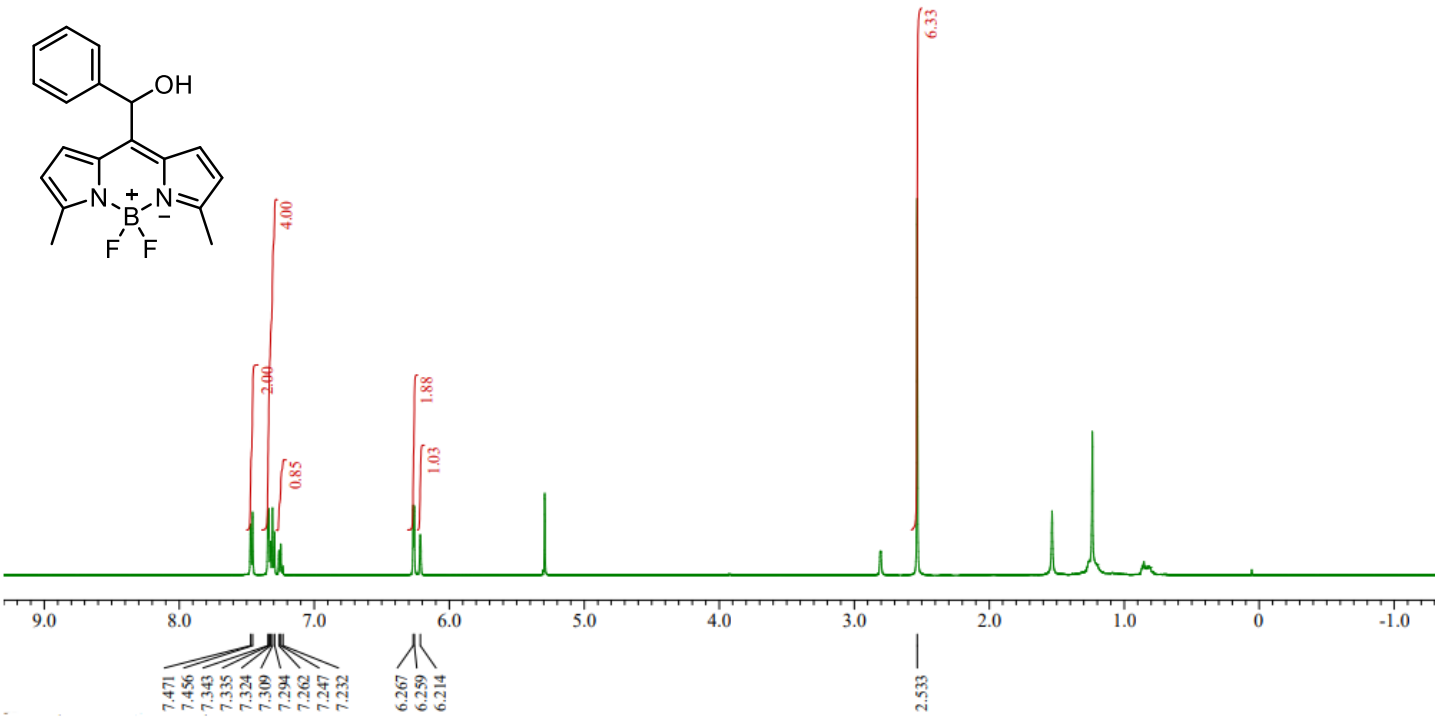

^{13}C-NMR Spectrum of **2-OH** in CD_2Cl_2 (100 MHz):

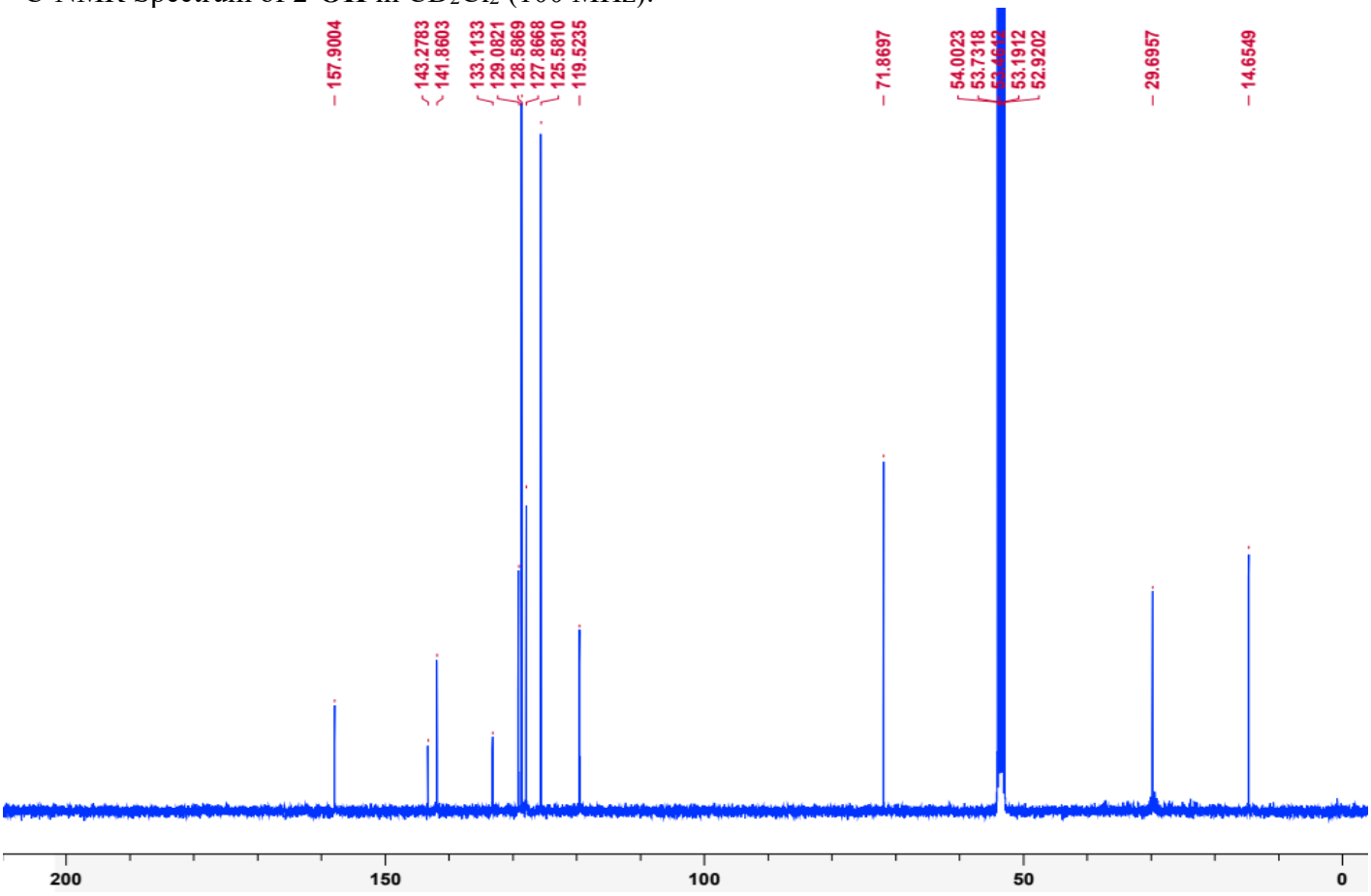

HR-MS Spectrum of **2-OH**:

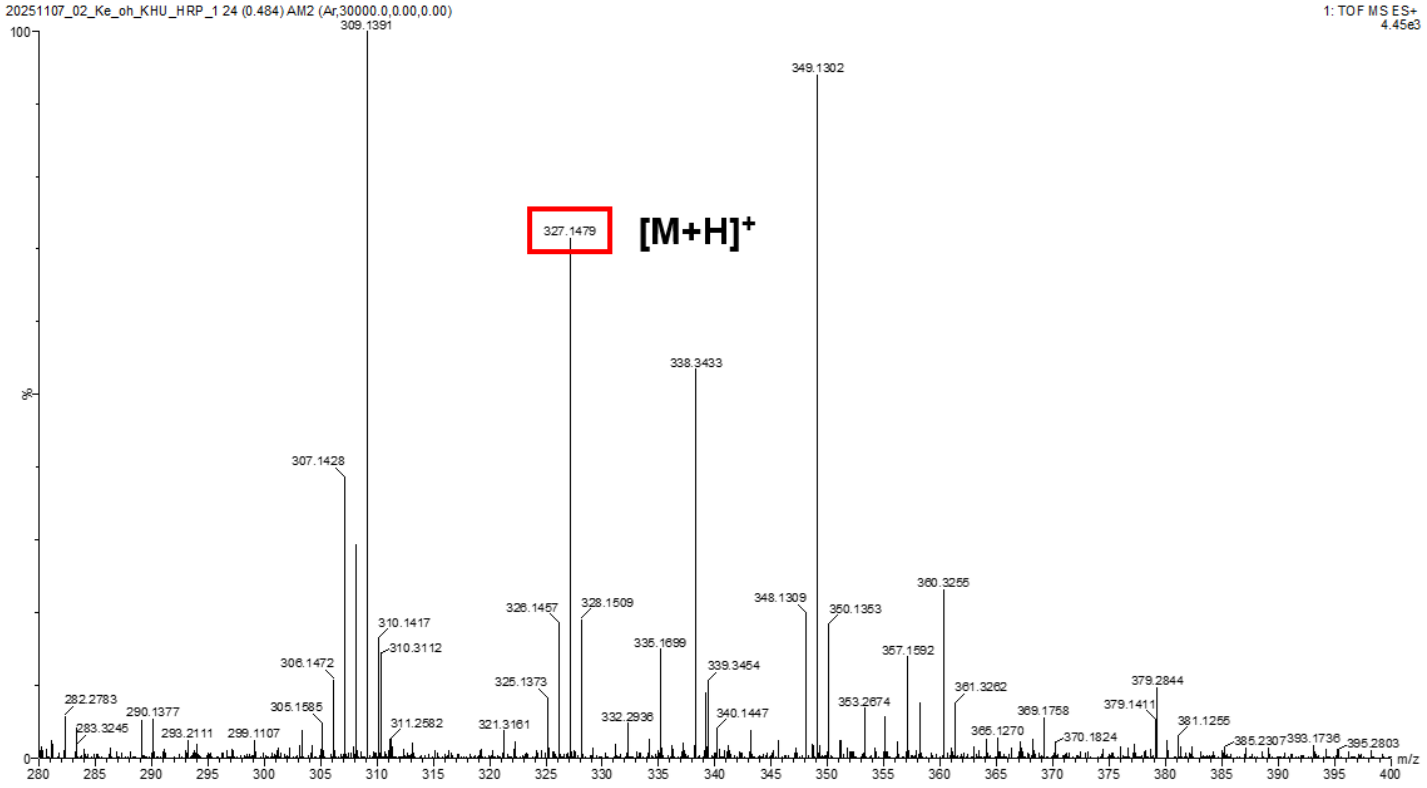

^{1}H-NMR Spectrum of **2-CO** in CD_2Cl_2 (500 MHz):

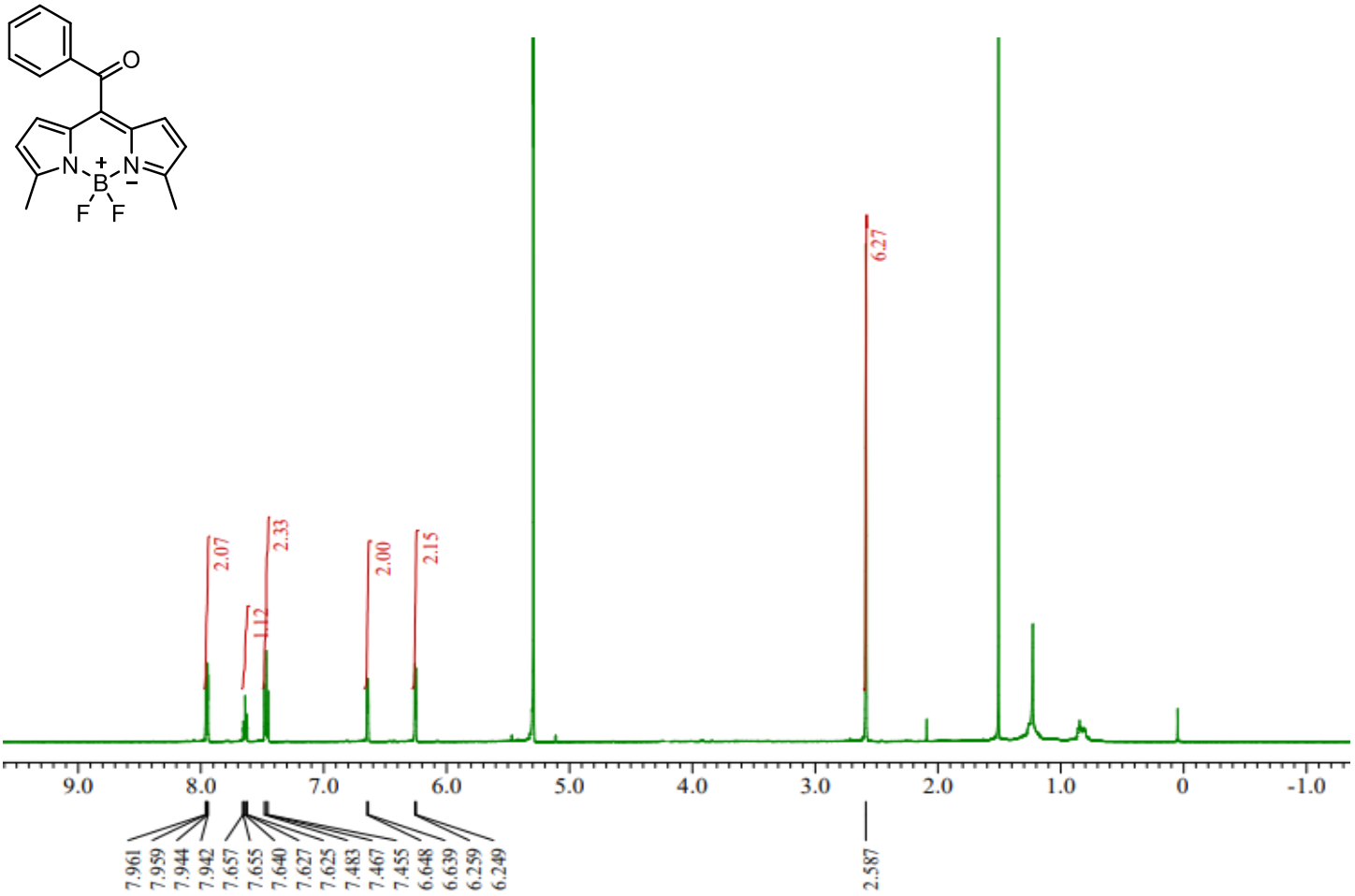

^{13}C-NMR Spectrum of **2-CO** in CD_2Cl_2 (100 MHz):

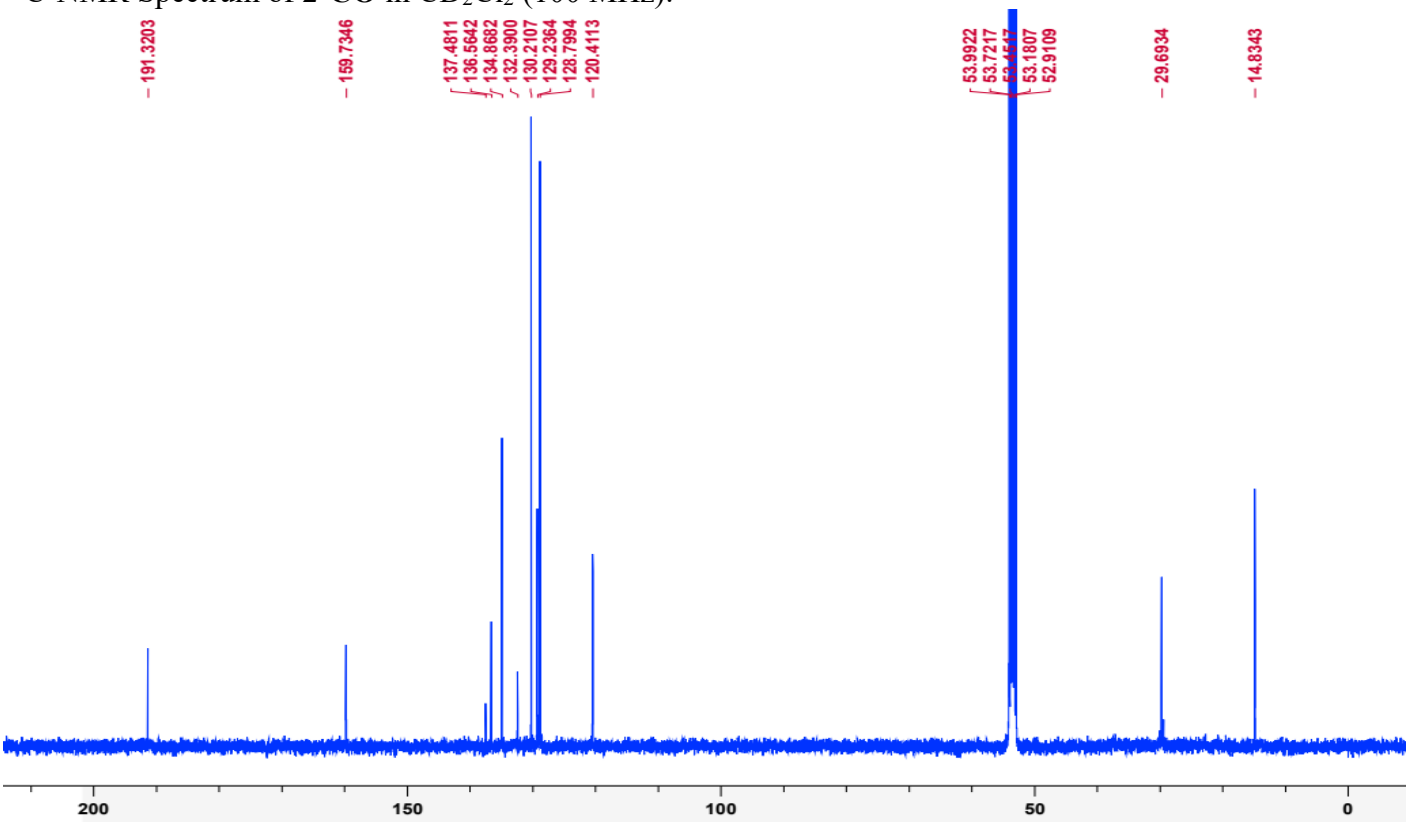

HR-MS Spectrum of **2-CO**:

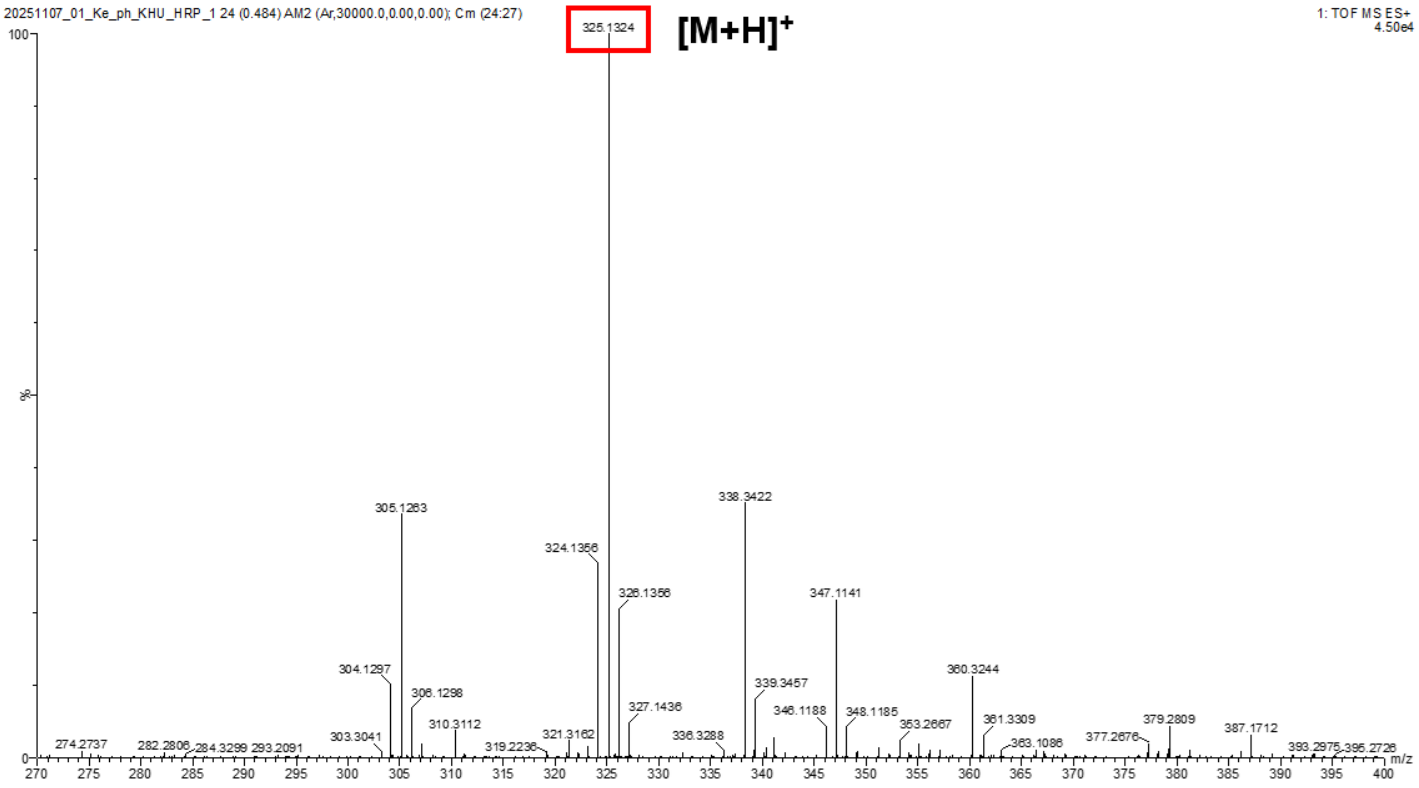

12. References

1 T. Slanina, P. Shrestha, E. Palao, D. Kand, J. A. Peterson, A. S. Dutton, N. Rubinstein, R. Weinstain, A. H. Winter and P. Klán, *J. Am. Chem. Soc.*, 2017, **139**, 15168.

2 Y. Kim and Y. Kim, *Org. Lett.*, 2025, **27**, 6710.

3 M. T. Whited, N. M. Patel, S. T. Roberts, K. Allen, P. I. Djurovich, S. E. Bradforth and M. E. Thompson, *Chem. Commun.*, 2012, **48**, 284.

4 T. M. Penning, M. E. Burczynski, J. M. Jez, C.-F. Hung, H.-K. Lin, H. Ma, M. Moore, N. Palackal and K. Ratnam, *Biochem. J.*, 2000, **351**, 67.

5 R. Thomsen and M. H. Christensen, *J. Med. Chem*., 2006, **49**, 3315.

6 PerkinElmer Informatics. Chem3D 15.0 User Guide. Waltham, MA: PerkinElmer Inc.; 2014.